The Metabolomics Profiling of Chronotherapeutic of Synergized Structure Nano-Lipid Honey- PDGF in Rabbit Wound Healing

Noor Thabit Nouman[*] and Mohanad A. Al-Bayati[*]

[*]Department. of Physiology and Pharmacology, College of Veterinary Medicine, Baghdad University.

[1] Department of Physiology, Biochemistry, and Pharmacology, College of Veterinary Medicine, University of Baghdad, Iraq

[2] Department of Physiology, Biochemistry, and Pharmacology, College of Veterinary Medicine, University of Baghdad, Iraq

*Corresponding author: aumnmumu@covm.uobaghdad.edu.iq

Abstract. Chrono-therapeutics tries to adapt therapies to 24-hour rhythms, which come about as a result of the circadian timing system's regulation of the majority of biological functions. In order to achieve maximum healing perfection by using Nano lipid-carried nutraceuticals with orchestrating between healing phases of honey and growth factor in modulating their concentration and profiling of metabolomics fact of wound healing during treatment, a more novel chrono-pharmacological statement of Nano lipid application in a different time is required. Chronopharmaceutical possible to optimize pharmacotherapeutics while taking into account rhythm dependencies in the kinetics and dynamics of drugs, which is predicted in temporal variability for skin and wound healing. Patients and Methods: Twenty-five rabbits were endorsed in the present study divided into five groups. The full excisional wounds were treated with different formulas, control group and $SNL_{Honey\ \&\ PDGF}$ treated groups which were divided according to effective concentration EC_{50} and EC_{20} as follows ($EC_{50Honey}$ 11.97 & EC_{50PDGF} 0.38, $EC_{50Honey}$ 11.97 & EC_{20PDGF} 0.08, $EC_{20Honey}$ 1.16 & EC_{50PDGF} 0.38, and $EC_{20Honey}$ 1.16 & EC_{20PDGF} 0.08%) respectively, as a daily dressed treatment. The linear closure rate of wound healing t½ and closure velocity were measured, choosing the best effective concentration of honey and PDGF. After that, fifty rabbits were divided according to the treatment diurnal time (7, 15, and 23) into four major groups: control, SNL-blank, conventional $EC_{50Honey\ \&}$ $EC_{20\ PDGF}$, and SNL $EC_{50Honey\ \&}$ $EC_{20\ PDGF}$. Results: The outcomes of wound healing demonstrated the quality and extent of synergism between the effective concentrations of $SNL_{Honey\ and\ PDGF}$. Also, compared to conventional and SNL-blank forms, the chrono-therapeutic challenge of synergistic $SNL_{Honey\ and\ PDGF}$ lowered wounds and was faster healed. In addition to the fold changes of metabolomes in Chrono protocolled treated groups of skin wound healing Succinic acid 0.86, Fumaric acid (Dimethyl fumarate) 1, beta-Sitosterol acetate 1, 2-Deoxy-D-galactose 1.28, Proline 1, Arginine 1.06, Adenosine 1, Xanthine (Purin-2,6-dione) 2.6, alpha Tocopherol 1, and Phosphoramidic acid 1, the diagnostic markers of metabolomes, in dosed during a significant appearance or disappearance and increase or decrease metabolomes fractions determined according to groups marker differentiation between treated groups: control and SNL-Blank Succinic acid and Fumaric acid (Dimethyl fumarate), SNL-Blank and conventional beta.-Sitosterol acetate and 2-Deoxy-D-galactose, and conventional and $SNL_{Honey\ and\ PDGF}$ Proline, Arginine, Adenosine, Xanthine (Purin-2,6-dione), alpha Tocopherol, and Phosphoramidic acid. Conclusion: The combination of $SLN_{Honey\&\ PDGF}$ according to effective concentration increased of synergism of honey and PDGF and therefore accelerated wound healing. The Chrono-therapeutic effect led to optimized results to increase the efficiency of the therapeutic effect via utilizing circadian rhythm through identifying a class of biomarkers that correspond to wound healing processes.

Keywords: Structural Nano Lipid, wound, chronotherapeutic, metabolomes, honey, Platelet derivative growth factor, Rabbit.

1. Introduction

One of the health issues that compromises skin integrity is wounds. Wound healing varies and fluctuates due to many internal and external microenvironmental elements that have an impact on the healing process (Monika *et al*., 2021). The pharmaceutics care agents on skin wounds were subjected to various maneuvers and determined optimized remedies; via various protocols, the new scientific approaches excreted Nanopharmaceutics; a special Nano lipid delivery system to increase stability, control, and release of drug as well as drug targeting sites, reduce bolus dosage, improve pharmacokinetic bioavailability, biodegradability, protect of labile drug against chemical degradation, the incorporation of nanoparticles into the delivery system, and (Campos *et al.*, 2020).

Also, contemporary pharmaceutical businesses set up sites to gather data and minimize dose delivery. Several medications are combined in standardized dosage forms through the synergism interaction to reduce the dose, reduce toxicity, and boost potency and efficacy (Araujo *et al.*, 2020). Optimal results of the pharmaceutics challenge were set at a specific time of treatment to increase the effectiveness of therapeutic effect by utilizing circadian rhythm as managed within chrono-pharmacology, which was useful to monitor therapy, to limit the duration of therapy, makes the use of the drug more appropriate, prevents an overdosing of the drug, and decreases thus the side effects of a drug (Devdhawala and Seth, 2010).

Metabolomics is one of the controlled treatment efficiency monitors. It is a thorough assessment of the recognizable chemical fingerprints of tiny molecule metabolites within the living process (cells, tissues, in addition to body fluids). The metabolomics-derived markers were authorized for healing characteristics and end-of-remodeling in addition to providing a diagnostic tool with clinical applicability. Superior wound healing and maximum remodeling are provided by the itemized portion of Nanopharmaceuticals of formulated honey and PDGF difficulties optimizing synergism with chrono-pharmacology and advise (Wang *et al.*, 2018).

The study aims to curable wounds with minimized impact adverse effect by determining chronotherapeutics of synergistic Nano lipid carrying growth factor and honey under basic concept chronopharmacological spectrum.

2. Methodology of the study

2.1. Experimental design

Twenty-five rabbits were divided into five groups, which treated the daily application as follows negative control group and $SNL_{Honey\ \&\ PDGF}$ treated groups which were divided into four subgroups according to effective concentration EC_{50} and EC_{20} infiltrated in the skin for achieved dosing of the dose-response curve components, which represented as follow ($EC_{50Honey}$ & EC_{50PDGF}, $EC_{50Honey}$ & EC_{20PDGF}, $EC_{20Honey}$ & $EC_{50PDGF,}$ and $EC_{20Honey}$ & EC_{20PDGF}) respectively. The chronotherapeutic challenge of synergistic $SNL_{Honey\ and\ PDGF}$ formulas on deep skin wounds in rabbits, after choosing the best effective concentration of honey and PDGF from experimental I.

Fifty rabbits were divided into four major groups (1st negative control, 2nd positive control SNL- blank, 3rd conventional $EC_{50Honey\ \&}$ $EC_{20\ PDGF}$, and 4th SNL $EC_{50Honey\ \&}$ $EC_{20\ PDGF}$). Each group was divided into three subgroups according to the treatment diurnal time (7, 15, and 23) after challenging the superlative time in Chronopharmacology for wound healing and skin restoration.

2.2. Preparation of $SNL_{Honey\& PDGF}$

According to Zhang *et al.* (2018), the solvent diffusion method was used to prepare the structures Nano lipid. The formulation involved forming the lipid status from stearic acid that had been dissolved in glycerine monostearate and then dispersing it with 2 ml of castor oil at 800 rpm for 30 minutes. In order to reach concentrations in 1ml of dimethylformamide and dispersion at 800 rpm for 30 minutes, the developing lipid phase was also dissolved in phosphatic acid and loaded in the necessary quantity with honey or PDGF. Following that, dispersion at 800 rpm for two hours while adding a dissolving form to the lipid form (Nawal *et al.*, 2020; Buthina and Mohanad, 2023).

Additionally, the gel was created by dissolving 0.125g of carbopol in 3ml of distilled water and stirring to form the gel phase. The gel's acidic component was then balanced by adding 1ml of NaOH 0.1N and mixing thoroughly until the suspension thickened and became clear. The gel was then heated for 15 minutes to remove any remaining air bubbles before SNL honey or PDGF was added to the gel at 0.3g v/w (Roaa and Mohanad, 2022).

2.3. Synergism and antagonism between agents

According to Berenbaum, (1989), the type of interaction between agents could be determined by using the following formula:

$d_a/ D_a + d_b/ D_b < 1$ ……. Synergy effect

$d_a/ D_a + d_b/ D_b = 1$ ……. Zero interaction

$d_a/ D_a + d_b/ D_b > 1$ ……. Antagonist effect

Where d_a and d_b are the concentrations of drugs A and B used in combination and $D_{a\ and}$ D_b are their single concentrations, which were effective with the combination ($d_a + d_b$) at any specified level of effect (Ali and Mohanad, 2020). Then if there were synergistic effects between some agents we calculated the degree of synergism according to Poch and Holzmann, (1980), by using the following equation:

$$E_{A+B} = E_A + E_B - (E_A \times E_B)$$

The theoretical curves for response might be produced using a spreadsheet where E can be stated as a fraction of the maximal effect (1.0), using this equation and the data for the experimentally obtained relaxation for drugs A and B.

2.4. Induction of excisional wound in skin

Each group was anesthetized with subcutaneous infiltration of lidocaine 2% local anesthetic formulation, according to the ethical as placebo fact Balbino *et al.* (2005).

2.5. The surgical wounds creation

The prepared surgical site and skin were labeled about 0.8 cm as a circular line, the skin fold at para-Medline and the dorsal parts were raised cranially and caudally by using thumbs, and the sterile biopsies were removed on half-circular skin folds by the surgical blade to completely remove whole skin layers and part of muscle, resulting in symmetrical excisional wounds (Camila *et al.*, 2015; Bruno *et al*., 2020).

2.6. Wound closure monitoring

The wound area of monitored rabbits was evaluated until the wound closure area was completed, and the dimensional diameters of the wound area were measured on days 5, 10, 20, and 30 as follows:

$$wound\ area = \frac{diameter A}{2} \times \frac{diameter\ B}{2} \times \pi$$

Furthermore, Gopinath *et al.* (2004) used the following equation to calculate the percentage of kinetic wound closure:

$$wound\ closure = \frac{actual\ wound\ area\ (cm)}{Initial\ area\ of\ wound} \times 100$$

Following that, the new tissue formation was analyzed, and slices were evaluated to encompass the healing wound borders (the area of wound boundary between the edge of intact connective tissue and the one of new tissue formation) and the wound center or the forming scar. Cassini et al. (Cassini *et al.*, 2015; Roaa and Mohanad, 2022) examined the wounds and five slices and calculated wound closure indices based on three parameters:

1. **Closure rate**: the skin wound closure area per unit time during the total growing phase, as calculated by:

$$Closure\ rate = \frac{1-\frac{Intial\ wound\ area-final\ wound\ area}{intial\ wound\ area}}{Time\ (days)}$$

2. **Closure velocity**: the total time required for wound closure as calculated by the following equation(Gilman, 2004):

$$Closure\ velocity = \frac{\Delta A_{\ i-f(primeter)}}{\Delta t}$$

   * $\Delta A_{\ i-f}$ the change between the area of the excisional wound and the final closure area,

3. **T½ of wound healing**: the half-life of wound closure area time in treated groups, as calculated by equation (Vidal *et al*., 2015):

$$t½\ closure = \frac{q}{Dc}: \text{where}\quad Dc = \frac{\Delta r}{\Delta t}$$

*q is the intercept, ΔA= change alter in apparent wound area between two consecutive times of measurement, Dc continuous linear healing rate, Δt= Time between two certain consecutive measurements

2.7. Tissue collection

To estimate some biochemical parameters such as protein concentration and DNA extraction, tissue was excised from each wound at time intervals of (7, 15, and 23) taken after wound healing.

2.8. Measurement of tissue protein concentration at full closure wound the specimens

Using a chilled pestle and mortar and a pinch of glass wool, the tissue (30 mg) was pulverized in ice-cold lysis buffer containing 100 mM Tris-HCl, 0.05 mM EDTA in a proportion of 300 l of lysis buffer/30 mg tissue. The homogeneous mixture was transferred to a 1.5 ml microcentrifuge tube and centrifuged for about 10 minutes at 10000 rpm after pulverization. Protein concentrations in supernatant protein lysate were calculated (Lowry *et al.*, 1951).

2.9. Measurement of DNA extracted

Extraction and estimation of DNA using the phenol-chloroform method with some modifications (Sambrook and Russell, 2001) Homogenize the tissue in liquid nitrogen using a motor pestle.

- Add 600µl of ice cold cell lysis buffer (10mM Tris-HCl, pH=8, 0.3028gm/250ml, 1mM EDTA, 0.09306gm/250ml, 0.1% SDS, 0.25gm/250ml) and thoroughly mix by vortexes.
- Incubate 2.5µl Proteinase K (20mg/ml) at 65°C for 1 hour, followed by 15 minutes at 95°C (or incubate at 50c overnight).
- An equal volume of Saturated Phenol (pH 8.0); thoroughly mix for 10 minutes with gentle inversions. After that, I used a centrifuge at 14,000 rpm for 5 minutes at 40oC to gently remove the upper aqueous layer and transfer it to a new tube.

- Phenol was softly mixed in an equal volume. Chloroform: Isoamyl alcohol (25:24:1), centrifuged at 14,000 rpm for five minutes at 40°C, and the upper aqueous phase was collected into a new tube.
- Chloroform: Equal volumes of isoamyl alcohol (24:1) are added, and the upper aqueous phase is removed into a fresh tube after centrifuging at 14,000 rpm for five minutes at 40C.
- Add 150 µl of potassium acetate (60 ml, or 29.44 g/60 ml) along with 11.5 ml of glacial acetic acid and 28.5 ml of DH2O, and thoroughly mixed.
- Next, add the same amount of isopropyl alcohol or isoamyl alcohol. 500 µl of 70% ethanol was added to the DNA pellet after being centrifuged at 14,000 rpm for 5 minutes at 40°C. Centrifuge at 40°C for 5 minutes at 14,000 rpm.
- Carefully removed the supernatant and let the DNA pellet air dry before dissolving it in 100 µl of 1X TAE buffer at 65°C for an hour (or keep overnight at room temperature).
- The DNA samples are divided into aliquots and kept at 20°C for later use. A spectrophotometer was used to find the amount of DNA (Hitachi-U-1800).

2.10. Blood collection

For metabolomics, blood was collected from rabbits by direct ear puncture from each wound at time intervals of (7, 15, and 23), 6 ml of blood were drawn and placed right into a frizzed K3EDTA tube. To separate plasma from blood cells, a spare tube was spun at 4000 rpm for 5 minutes. To instantly freeze the sample, plasma is kept in Eppendorf tubes and preserved in liquid nitrogen. Dry ice was utilized for transit to the laboratory (Li *et al.*, 2017).

While in the hormonal assay, the blood was transferred to the plain tube and let to clot, and centrifugation for 5 minutes to separate the serum and transfer to the Eppendorf tube then the tubes were kept in a freeze at 8ºC until estimated some hormones by Radioimmunoassay technique such as Melatonin (Maurya and Chronopharmacology, 2012), Growth hormone (Evans *et al.*, 1980), Thyroid stimulating hormone (TSH) (Hepburn *et al.*, 2012), Cortisol (Roberts and Roberts, 2004) and Insulin (Li *et al.*, 2017). Use the correlation coefficient formulas in experimental three for determined a significant incidence of high degree in the dosed protocol (Armitage and Berry, 1994).

2.11. Metabolomics profiling

A mass spectrometer and an automated pyrolysis gas chromatography were used to perform GC-MS analysis for metabolomics (Trezzi *et al.*, 2016; Ali and Mohanad, 2019). Using a GC/MS total ion chromatogram to represent each sample, the peaks in the chromatograms were recognized using the NIST mass spectral library, and the peak areas for each drug were calculated based on their relative levels to the control group using the equation below (Fiehn and Kind, 2005).

$$\text{"}Relative\ level\ of\ metabolite\ (fold\ change) = (sample\ areas - control\ area)/\ (control\ area) * 100$$

In order to compare the levels of metabolites in the treatment and control groups and identify any differences, multivariate statistics (Fratio of variance) were calculated after converting the value to Log10. The differences between the groups were deemed statistically significant when the P-value was less than 0.05. (Jassim, and Bayati, 2019).

2.12. Ethics

For handling and management of rabbits, the ethics were based on the AUCUC protocol "Laboratory Animal Care and Use Guidelines for Research and Education," as well as ethical craft pharmacological dosing and cure maneuvers according to Al-Bayati and Khamas, (2015).

2.13. Statistical analysis

The data results in analyses were done via Windows Microsoft Excels program for F test (ANOVA) one way and two ways according to the experimental outcome and results requirement. LSD tests were used in statistical analysis for the study the control and treated groups were subjected to analysis two of variance a probability of $p< 0.05$ was assumed to denote a significant difference. LSD test has used a comparison between groups and time for identified significance data. Log dose-response curve and their parameter were calculated, binomials curve, and plotted by software Excel prepared by Tome O'Haver, (2015).

2.14. Results

2.14.1. Synergistic effect between $SNL_{Honey\ and\ PDGF}$ formulas wound closure time

The depiction represented in figure 1 displayed the synergistic model of the mixed drugs SNL $EC_{Honey\text{-}PDGF}$ Gel effect on timelines in wound healing phases; growth and remodeling were indicative of closure time area indices on time-dependent in the induced wound. The time reduction of wound recovery was significant ($p\leq0.05$) decrement ordered as follows:

($EC_{50\ honey\ +}\ EC_{20\ PDGF} < EC_{20\ honey\ +}\ EC_{50\ PDGF} < EC_{50\ honey\ +}\ EC_{50\ PDGF} < EC_{20\ honey\ +}\ EC_{20\ PDGF}$ < control)

The drive indices of wound closure were derived from the timeline of wound healing figure 2 expressed the indices of wound closure in $SNLEC_{50\ honey\ +}\ EC_{20\ PDGF\text{-}}$ Gel was significantly ($p\leq0.05$) higher than other dressed groups of $EC_{20\ honey\ +}\ EC_{50\ PDGF} < EC_{50\ honey\ +}\ EC_{50\ PDGF} < EC_{20\ honey\ +}\ EC_{20\ PDGF}$ < control respectively and as showed grossly in figure 3

As well as recording timeline curves of individual groups were displayed in figure 4 denoted to the points of curve behavior labeled the interactive between phases set velocity marker of the growing phase.

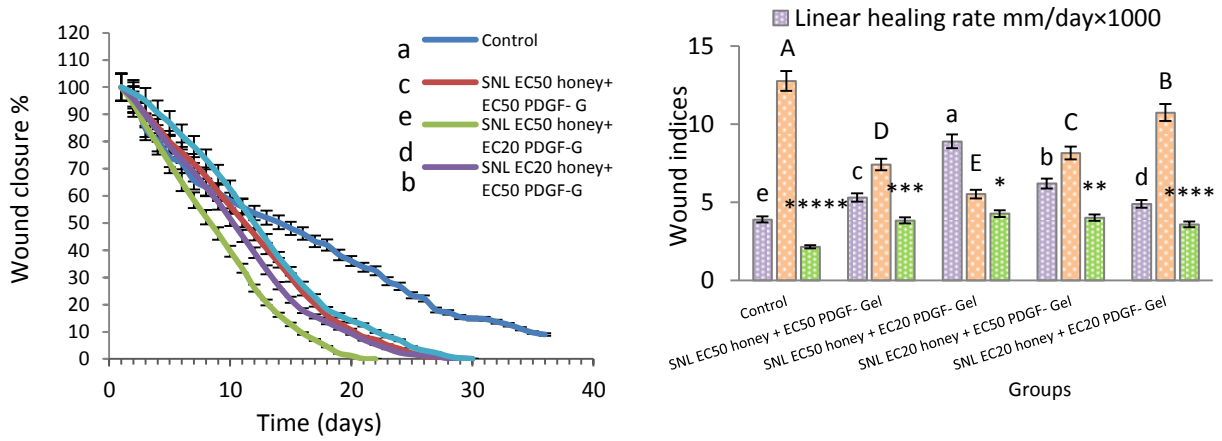

Figure 1. The timeline curve behavior of wound healing dressed SNL of honey-PDGF Gel as synergism. **EC_{50}**: Half Effective concentration, **EC_{20}**: Twentieth Effective Concentration, **PDGF**: Platelet-Derived Growth Factor, **SNL**= structure Nano lipid.

Figure 2. The wound healing indices in dressed wound groups by control and SNL of honey-PDGF- Gel syner
gism.

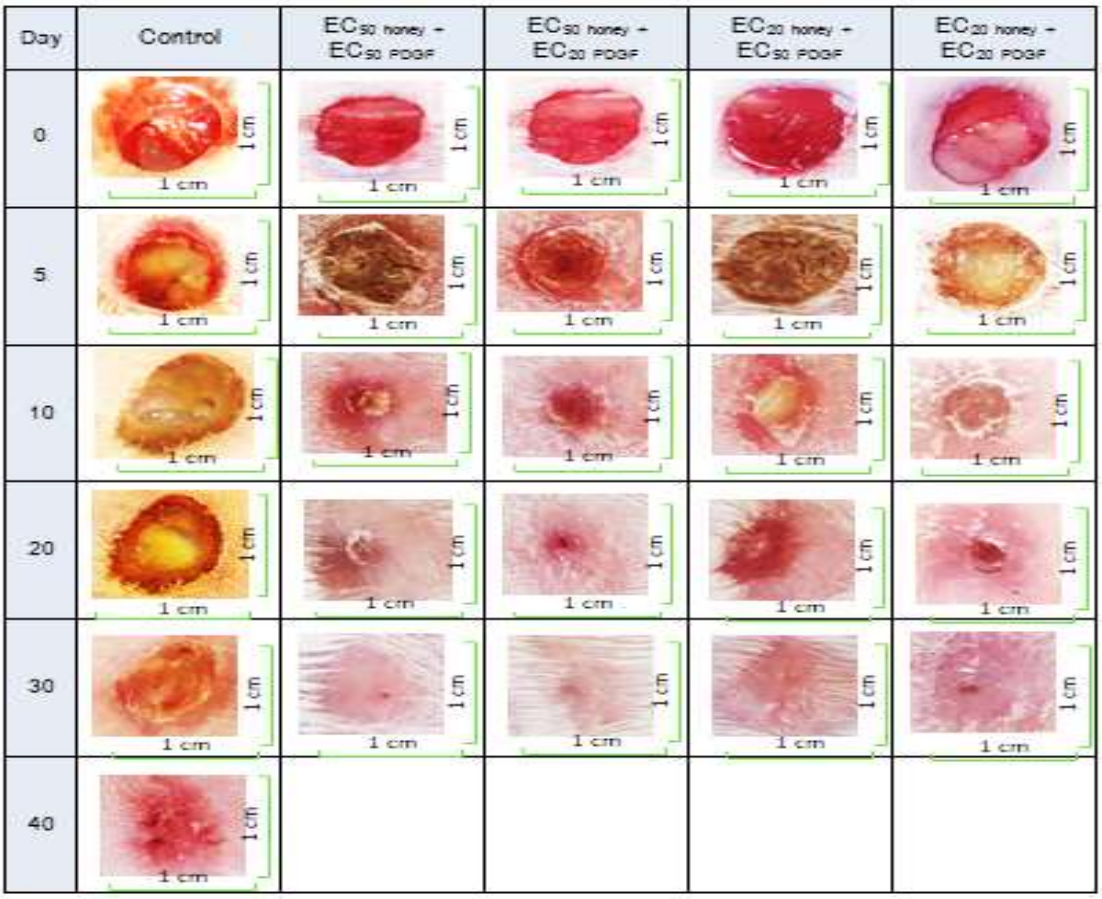

Figure 3. The depiction of wound grossly grow kinetic development in time track local treated by SNL of honey-PDGF- Gel synergism was observed according to ordered days

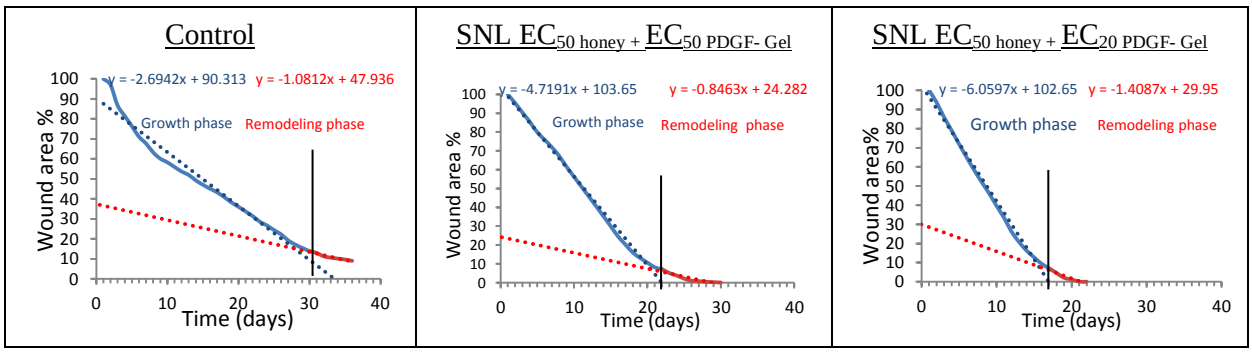

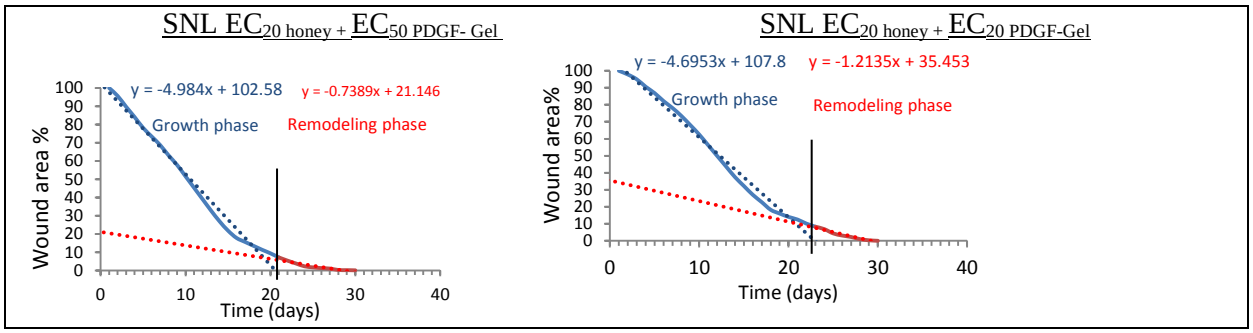

Figure 4. The comparison between wound healing kinetic curve of effective concentration in two-phase growing and remodeling phases in Structural Nano-lipid. **EC_{50}:** Half Effective concentration, **EC_{20}:** Twentieth Effective Concentration, **PDGF:** Platelet-Derived Growth Factor

2.14.2. Synergism quality and degree of effective concentrations (EC_s) SNL_{honey}-SNL_{PDGF} Gel in healing rabbits wounds

The SNL synergistic formulas were tabulated in pivot table 1 which were revealed to express all groups of the wound shared synergy less than < 1 and expressed the indices of synergism in all groups but SNL $EC_{50\ honey\ +}$ SNL $EC_{20\ PDGF-}$ Gel was significantly ($p \leq 0.05$) higher synergies degree than other dressed groups of $EC_{20\ honey\ +}\ EC_{50\ PDGF} < EC_{50\ honey\ +}\ EC_{50\ PDGF} < EC_{20\ honey\ +}\ EC_{20\ PDGF}$). As well as the degree of synergism was ordered significantly ($p \leq 0.05$) showing an increase of $EC_{50\ honey\ +}\ EC_{20\ PDGF}$ compared with other SNL $_{honey\ \&\ PDGF}$ formulas ($EC_{50\ honey\ +}\ EC_{20\ PDGF} <\ EC_{20\ honey\ +}\ EC_{50\ PDGF} < EC_{50\ honey\ +}\ EC_{50\ PDGF} < EC_{20\ honey\ +}\ EC_{20\ PDGF}$).

2.14.3. Chrono-therapeutic wound healing indices dressed by $SNL_{Honey\text{-}PDGF}$ and $Conventional_{Honey\text{-}PDGF}$ in healing indices

Figure 5 presented the Chrono-therapeutic effect on wound healing kinetic curve of synergistic formula SNL loaded honey-PDGF comparison with conventional honey-PDGF and SNL- blank at dose 11.97 and 0.08 challenge at 7:00, 15:00, and 23:00.

The closure indices in group SNL $_{honey-\ PDGF}$G at 23:00 dressed wound was butter than others groups treated at 15:00, whereas the reversed profile was seen in the conventionally treated group at 7:00 were showed at 7:00 the butter value of healing indices in the timeline than blank at 7:00.

2.14.4 The Chrono therapeutic of wound closure indices

The drive indices of wound closure were derived from the timeline of wound healing figure 6 expressed the indices of wound closure in $SNL_{honey-\ PDGF}$G at 23:00 was significantly ($p \leq 0.05$) higher than other dressed groups of conventional honey-PDGF and blank SNL respectively of linear healing rate and closure velocity, unlike timeline curve of closure $t_{1/2}$ increased SNL-blank at 23:00.

Table 1. The wound healing indices of Synergism quality and synergistic degree of effective concentrations (EC_s) SNL_{honey}-SNL_{PDGF} Gel.

Linear healing rate mm/day

Synergism

25 Rabbit		SNL Honey	
		EC_{20}	EC_{50}
SNL PDGF	EC_{20}	0.546	0.311
	EC_{50}	0.431	0.504

Degree of synergism

25 Rabbit		SNL Honey	
		EC_{20}	EC_{50}
SNL PDGF	EC_{20}	0.457 ± 0.17 C	10.625± 0.31 A
	EC_{50}	0.870± 0.14 B	10.430± 0.36 A

Closure $t_{1/2}$ days

Synergism

25 Rabbit		SNL Honey	
		EC_{20}	EC_{50}
SNL PDGF	EC_{20}	0.115	0.244
	EC_{50}	0.160	0.147

Degree of synergism

25 Rabbit		SNL Honey	
		EC_{20}	EC_{50}
SNL PDGF	EC_{20}	2.432± 0.27 d	12.518± 0.30 a
	EC_{50}	2.689± 0.22 c	10.719± 0.35 b

Closure velocity mm/day

Synergism

25 Rabbit		SNL Honey	
		EC_{20}	EC_{50}
SNL PDGF	EC_{20}	0.193	0.162
	EC_{50}	0.173	0.181

Degree of synergism

25 Rabbit		SNL Honey	
		EC_{20}	EC_{50}
SNL PDGF	EC_{20}	0.016± 0.006 ***	14.402± 0.27 *
	EC_{50}	0.337± 0.11 **	14.184± 0.32 *

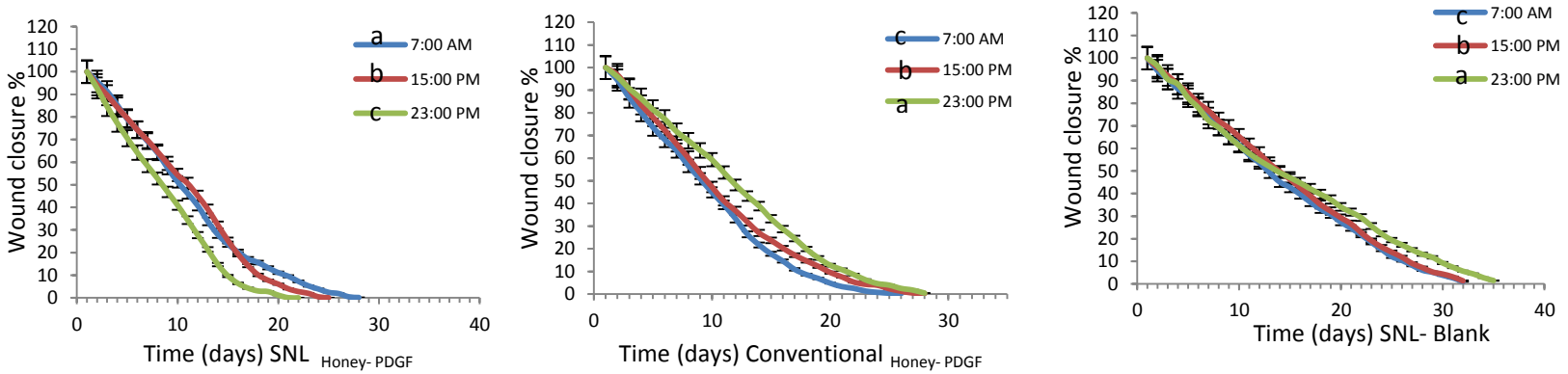

Figure 5. The timeline curve behavior of wound healing dressed SNL of honey-PDGF- Gel.

2.14.5. The protein concentrations of wound healing

The protein containing matrix composed protein as an indication of better healing was shown in figure 7 in Chrono preset point time of dressed synergistic formula of SNL, conventional honey and PDGF, and SNL-blank within growing and remodeling phases at 23:00, 7:00, and 15:00. The growing and remodeling phases was displayed higher significantly $p \leq 0.05$ protein concentrations at 23:00 6.018 and 7.324 respectively after dressed wound by the synergistic formula of SNL $EC_{50\ honey}$ - $EC_{20\ PDGF.}$

Furthermore, the second choice set time of improved healing was displayed in SNL $_{Honey\text{-}PDGF}$G at 7:00 4.14 and 6.11 respectively. The protein concentration was overcome the circadian oscillation and showed moderate to a low correlation in linear healing rate, closure $t_{1/2,}$ and closure velocity that make $SNL_{Honey\text{-}PDGF}$ synergized was modulate provoked protein synthesis due to their therapeutic activity rather than time oscillation as denoted in figure 8.

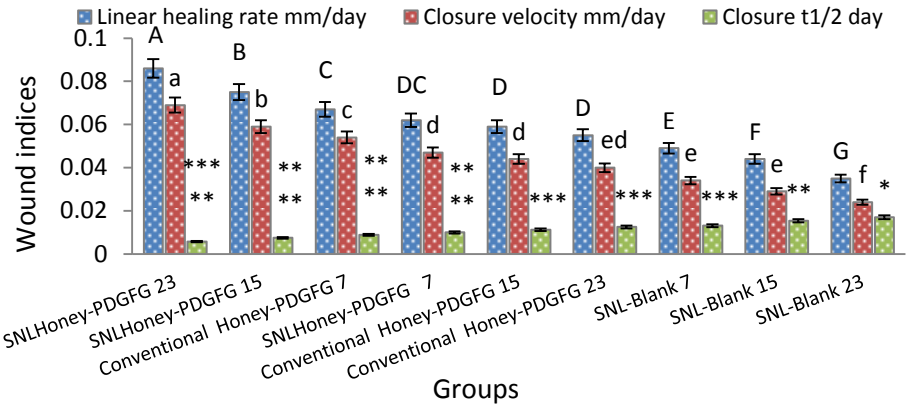

Figure 6. Timeline of wound area closure of induced circular wound treated topically with an effective concentration of honey and PDGF.

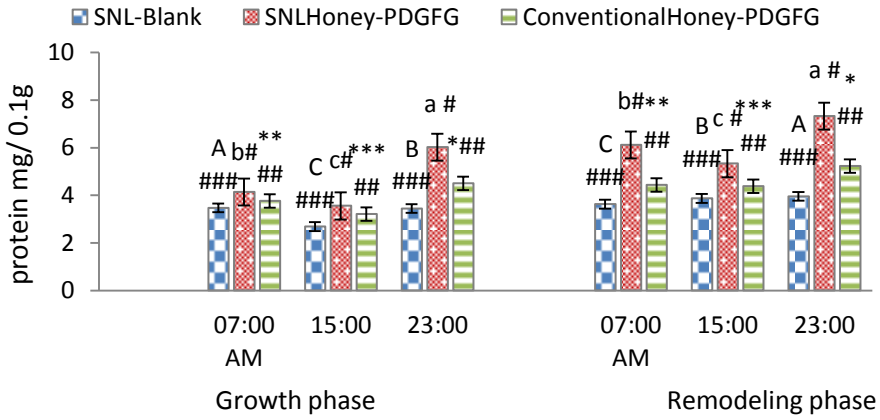

Figure 7. protein concentrations of the wound healing. The different capital, small leters and sign * refer to significant $p \leq 0.05$ between treated groups, # refer to significant $p \leq 0.05$ between time.

A. Growing phase

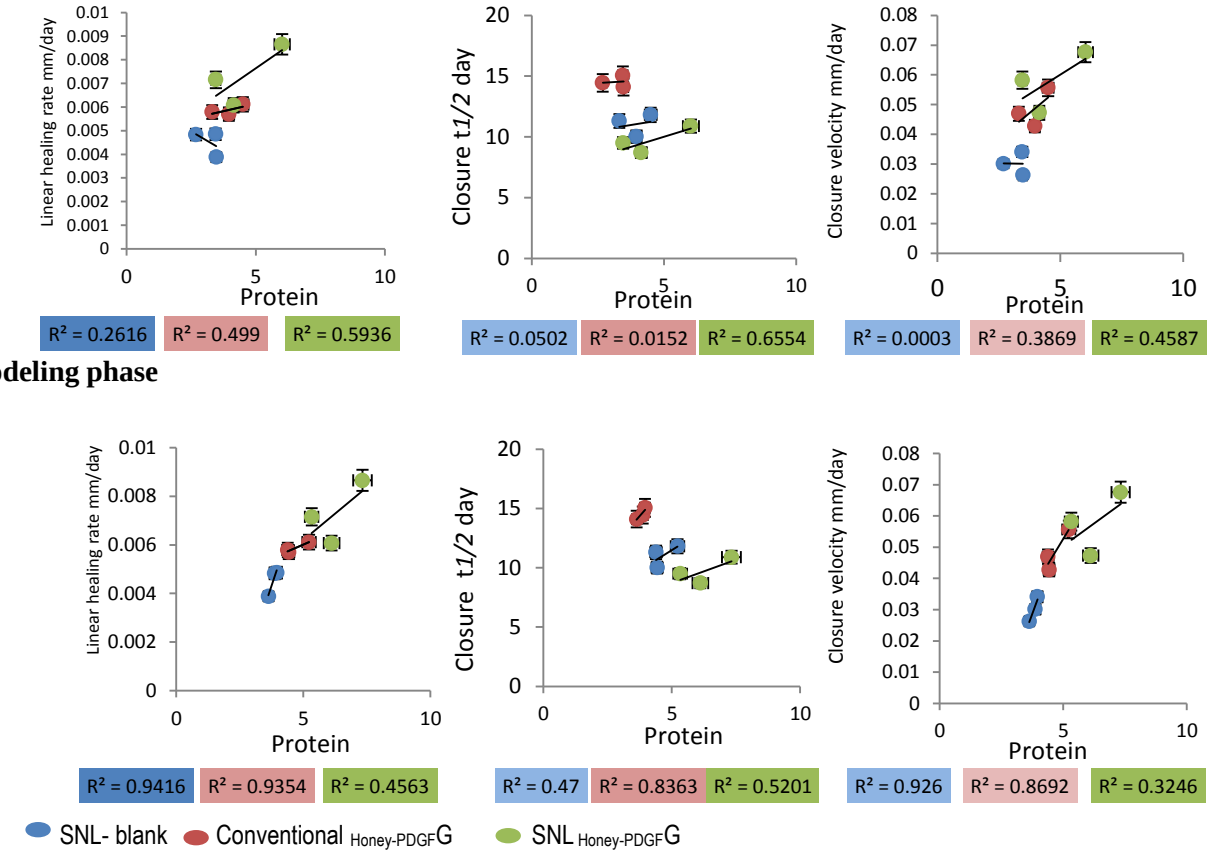

Remodeling phase

Figure 8. Correlation protein with wound indices in SNL-blank, SNL $_{\text{Honey-PDGF}}$G, and conventional $_{\text{Honey-PDGF}}$G.

2.14.6. The DNA concentrations of the healing wound

Another indication of cell building unit during the growing and remodeling phase was shown in figure 9 in Chrono preset point time of dressed synergistic formula of SNL, conventional honey and PDGF and SNL-blank at 23:00, 7:00, and 15:00. The growing and remodeling phases were displayed higher significantly $p \leq 0.05$ DNA concentrations at 23:00, 6.996 and 7.684 respectively after dressed wound by the synergistic formula of SNL $EC_{50\ \text{honey}}$ - $EC_{20\ \text{PDGF.}}$ Furthermore, the second choice set time of improved healing was displayed in $SNL_{\text{Honey-PDGF}}G$ at 7:00, 5.176, and 5.828 respectively. The DNA has in conventional high correlation with closure t½ negatively and less in velocity and linear healing rate positively and a high correlation with closure velocity negatively in the growing phase. While in remodeling high correlation in linear healing rate, closure $t_{1/2,}$ and closure velocity in conventional $_{\text{Honey\&PDGF}}$ and SNL-blank in linear healing rate, and closure velocity is positively seen in figure 10.

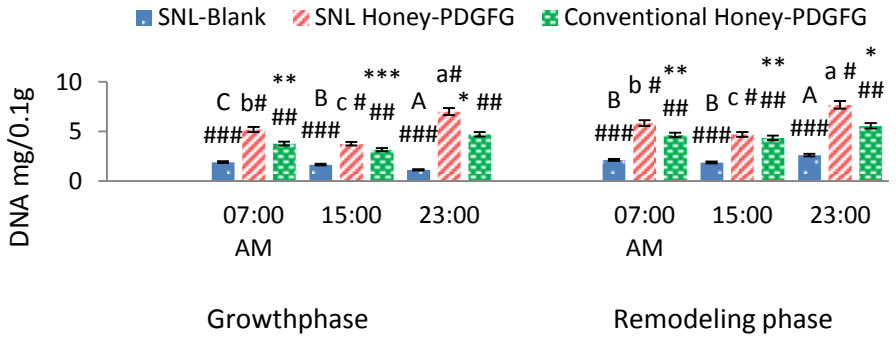

Figure 9. DNA concentrations of the wound healing. The different capital, small leters and sign * refer to significant $p \leq 0.05$ between treated groups, # refer to significant $p \leq 0.05$ between time.

A. Growing phase

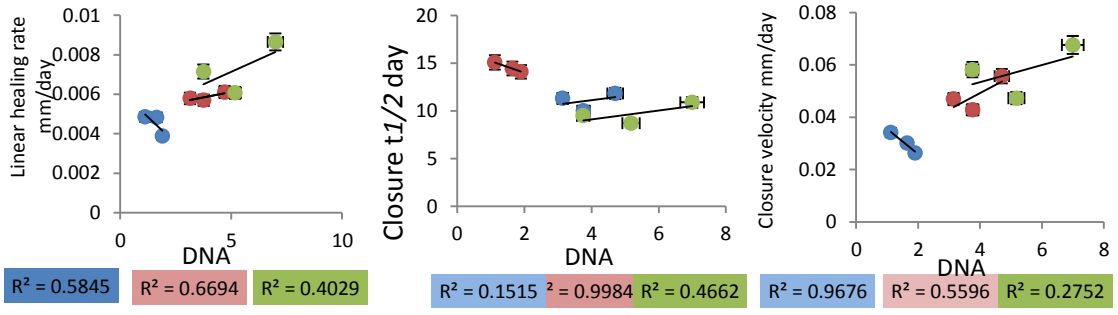

B.Remodeling phase

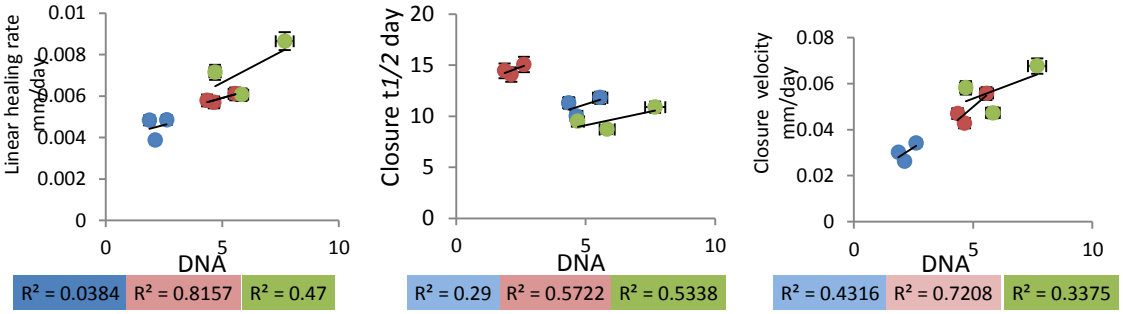

Figure 10. Correlation DNA with wound indices in SNL-blank, SNL $_{\text{Honey-PDGF}}$G, and conventional $_{\text{Honey-PDGF}}$G

2.14.7. The correlations of hormones with wound healing

The physiological concept of the diurnal rhythms was challenged in wound healing and the physiological term over the same factual directly turned of several hormonal could be managed in the dose of wound healing were displayed in figure 11 The placebo blank represented Benge's mark of standard conceptual directed covered wound healing. The evidence of a correlation the melatonin with hormonal changes was

highly relationship in all growth hormones and thyroid stimulating hormones, whereas insulin was highly correlated with melatonin in control and blank and friable in conventional and SNL Honey–PDGF but there was no evidence of outcomes correlation with cortisol in all given groups during wound healing.

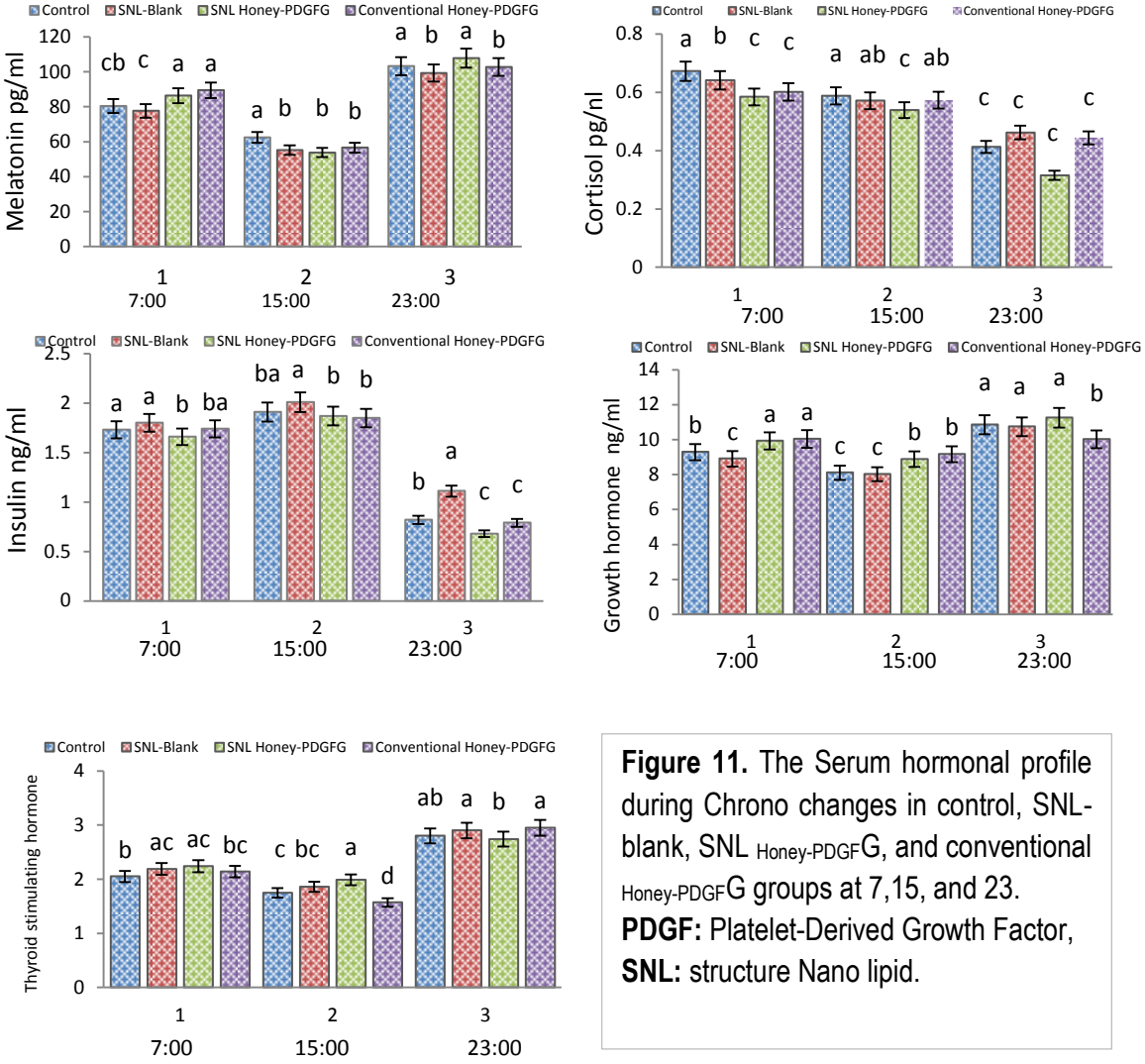

Figure 11. The Serum hormonal profile during Chrono changes in control, SNL-blank, SNL Honey-PDGFG, and conventional Honey-PDGFG groups at 7,15, and 23. **PDGF:** Platelet-Derived Growth Factor, **SNL:** structure Nano lipid.

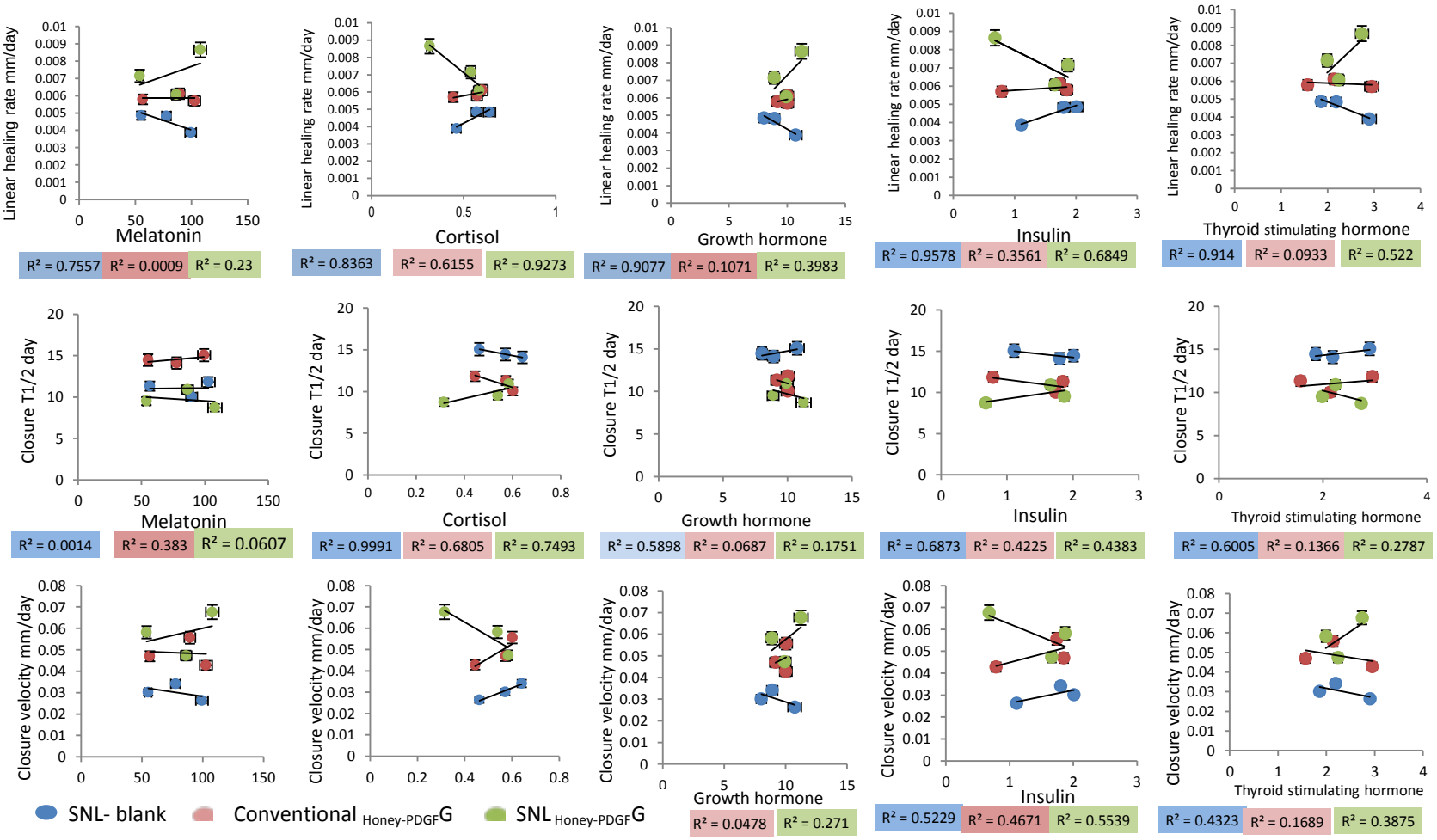

Figure 12. Correlation hormones with wound indices in SNL-blank, SNL $_{\text{Honey-PDGF}}$G, and conventional $_{\text{Honey-PDGF}}$G.

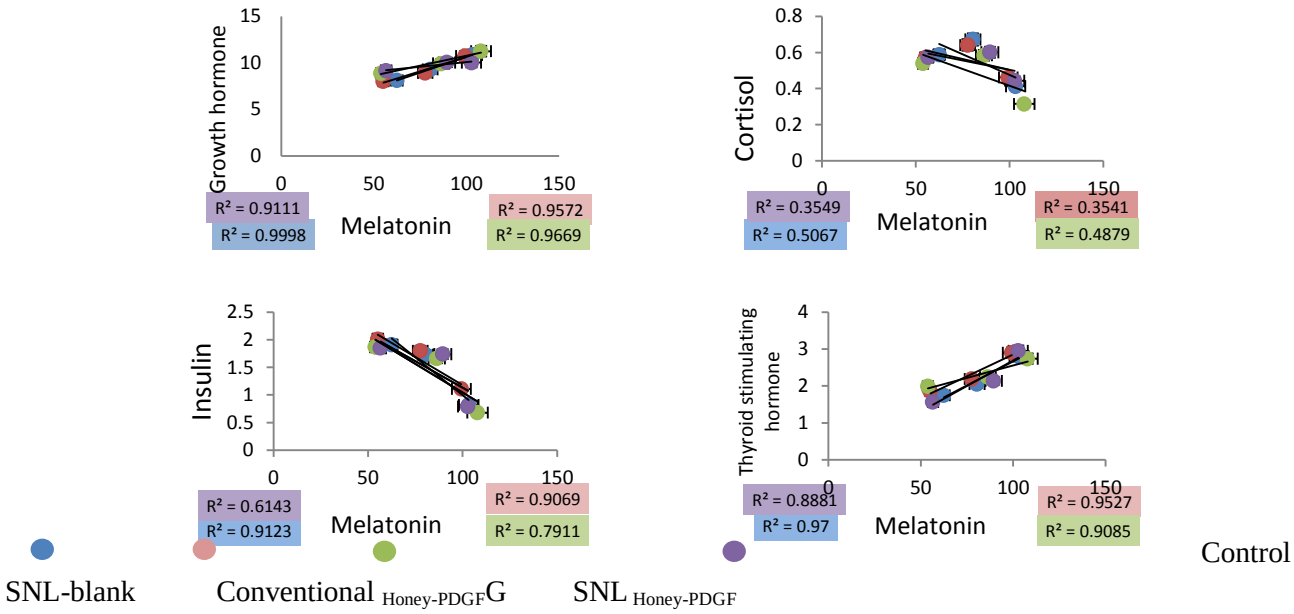

Figure 13. Correlation of melatonin with hormones in control, SNL-blank, SNL $_{\text{Honey-PDGF}}$G, and conventional $_{\text{Honey-PDGF}}$G.

2.14.8. Metabolomics profiling

The heat map of the metabolomics profiling as percent values of a healed wound skin at the remodeling phase in dressed groups SNL-Blank, Conventional$_{\text{Honey-PDGF}}$G, and SNL$_{\text{Honey-PDGF}}$G at Chrono therapeutics set 7:00, 15:00, and 23:00. The heat map exhibited several metabolome integrations in table 2 the total number of metabolomes 206 that driven form diversity of yield at Chrono set, which displayed the same numbers of the metabolome in SNL-Blank at 24 number at 7:00 treated groups as well as in 23:00, Conventional $_{\text{Honey-PDGF}}$G consist 25 metabolomes at 15:00 and 23:00 treated groups (p>0.05).

Figure 14 general numerate metabolome showed in control, SNL-Blank, Conventional $_{\text{Honey-PDGF}}$G, and SNL$_{\text{Honey-PDGF}}$G were 92, 78, 78, and 85 respectively, which were alienated according to time 7:00, 15:00, and 23:00 in control at 26, 39, and 27, SNL-Blank at 24, 30, and 24, Conventional $_{\text{Honey-PDGF}}$G at 28, 25, and 25, SNL$_{\text{Honey-PDGF}}$G 31, 28, and 26 respectively, and there were no significant between Conventional $_{\text{Honey-PDGF}}$G and SNL$_{\text{Honey-PDGF}}$G in 23:00. The difference within groups what found no significant between 15:00 and 23:00 in Conventional $_{\text{Honey-PDGF}}$G groups, in addition, there was no significant p>0.05 between 7:00 and 23:00 Chrono set treatment groups of SNL-Blank.

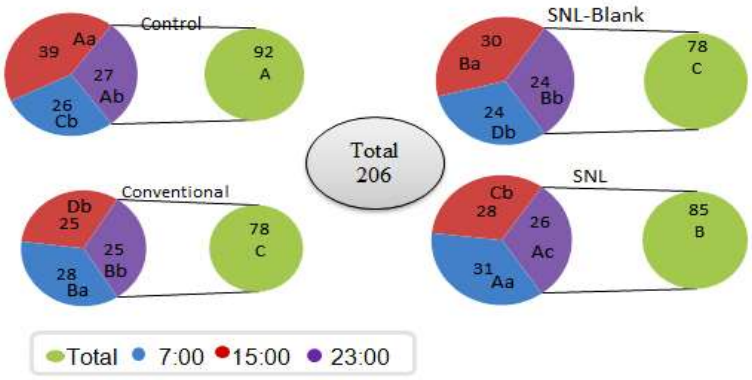

Figure 14. Total metabolomics profile in control, SNL-blank, conventional, and SNLHoney-PDGF. The data presented as mean ± SE, The different capital leters refer to different between groups and small leters refer to different between times significant p≤0.05.

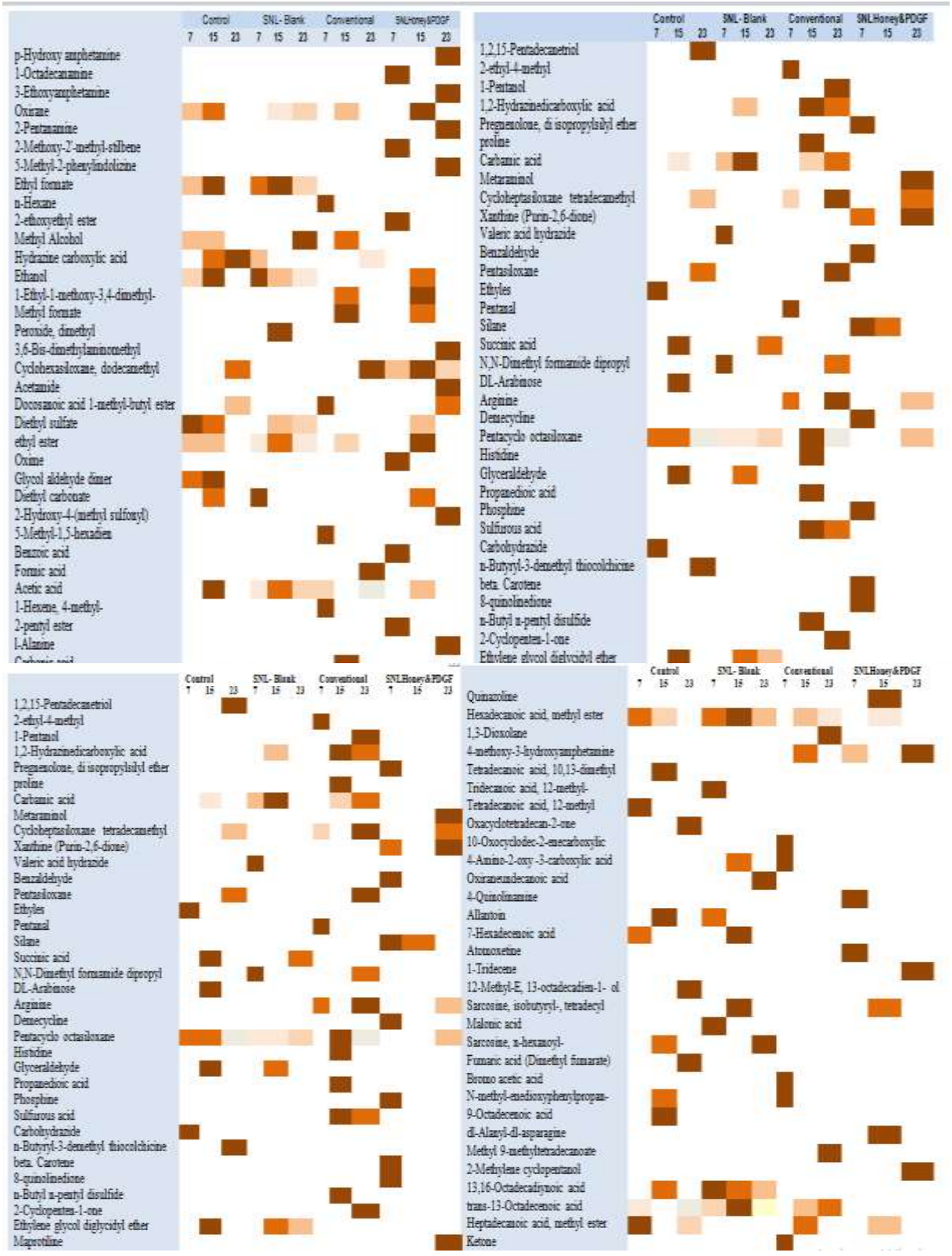
Control
SNL- Blank
Conventional
SNLHoney&PDGF
7 15 23
p-Hydroxy amphetamine
1-Octadecanamine
3-Ethoxyamphetamine
Oxirane
2-Pentanamine
2-Methoxy-2'-methyl-stilbene
5-Methyl-2-phenylindolizine
Ethyl formate
n-Hexane
2-ethoxyethyl ester
Methyl Alcohol
Hydrazine carboxylic acid
Ethanol
1-Ethyl-1-methoxy-3,4-dimethyl-
Methyl formate
Peroxide, dimethyl
3,6-Bis-dimethylaminoxanthyl
Cyclohexasiloxane, dodecamethyl
Acetamide
Docosanoic acid 1-methyl-butyl ester
Diethyl sulfate
ethyl ester
Oxime
Glycol aldehyde dimer
Diethyl carbonate
2-Hydroxy-4-(methyl sulfonyl)
5-Methyl-1,5-hexadien
Benzoic acid
Formic acid
Acetic acid
1-Hexene, 4-methyl-
2-pentyl ester
l-Alanine
1,2,15-Pentadecanetriol
2-ethyl-4-methyl
1-Pentanol
1,2-Hydrazinedicarboxylic acid
Pregnenolone, di isopropylsilyl ether
proline
Carbamic acid
Metaraminol
Cycloheptasiloxane tetradecamethyl
Xanthine (Purin-2,6-dione)
Valeric acid hydrazide
Benzaldehyde
Pentasiloxane
Ethyles
Pentanal
Silane
Succinic acid
N,N-Dimethyl formamide dipropyl
DL-Arabinose
Arginine
Demecycline
Pentacyclo octasiloxane
Histidine
Glyceraldehyde
Propanedioic acid
Phosphine
Sulfurous acid
Carbohydrazide
n-Butyryl-3-demethyl thiocolchicine
beta. Carotene
8-quinolinedione
n-Butyl n-pentyl disulfide
2-Cyclopenten-1-one
Ethylene glycol diglycidyl ether
Maprotiline
Quinazoline
Hexadecanoic acid, methyl ester
1,3-Dioxolane
4-methoxy-3-hydroxyamphetamine
Tetradecanoic acid, 10,13-dimethyl
Tridecanoic acid, 12-methyl-
Tetradecanoic acid, 12-methyl
Oxacyclotetradecan-2-one
10-Oxocyclodec-2-enecarboxylic
4-Amino-2-oxy -3-carboxylic acid
Oxiranenadecanoic acid
4-Quinolinamine
Allantoin
7-Hexadecenoic acid
Atomoxetine
1-Tridecene
12-Methyl-E, 13-octadecadien-1- ol
Sarcosine, isobutyryl-, tetradecyl
Malonic acid
Sarcosine, n-hexanoyl-
Fumaric acid (Dimethyl fumarate)
Bromo acetic acid
N-methyl-enedioxyphenylpropan-
9-Octadecenoic acid
dl-Alanyl-dl-asparagine
Methyl 9-methyltetradecanoate
2-Methylene cyclopentanol
13,16-Octadecadynoic acid
trans-13-Octadecenoic acid
Heptadecanoic acid, methyl ester
Ketone

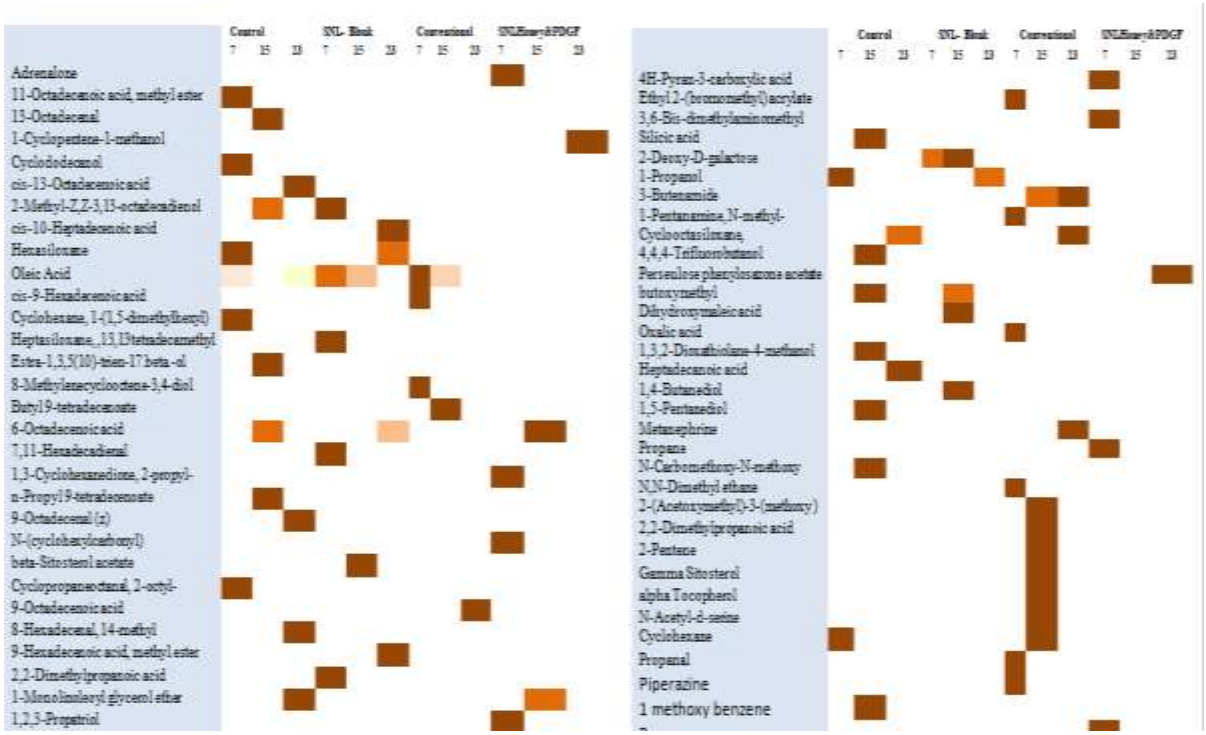

The schematic diagram 15 concludes the diagnostic markers of metabolomes, in dosed during significant appearance or disappearance and increase or decrease metabolomes fractions statically significant $p \leq 0.05$ determined according to g ps, in addition to the fold changes of metabolomes in Chrono protocolled treated groups of skin wound healing as shown in table 3.

Table 3. The fold changes of metabolomes in Chrono protocolled treated groups of skin wound healing

Compound	**Fold**
Shikimic acid	0.86
Fumaric acid (Dimethyl fumarate)	1
beta-Sitosterol acetate	1
2-Deoxy-D-galactose	1.28
Proline	1
Arginine	0.56
Arginine	1.06
Adenosine	1
Xanthine (Purin-2,6-dione)	2.6
Alpha Tocopherol	1
Phosphoramidic acid	1

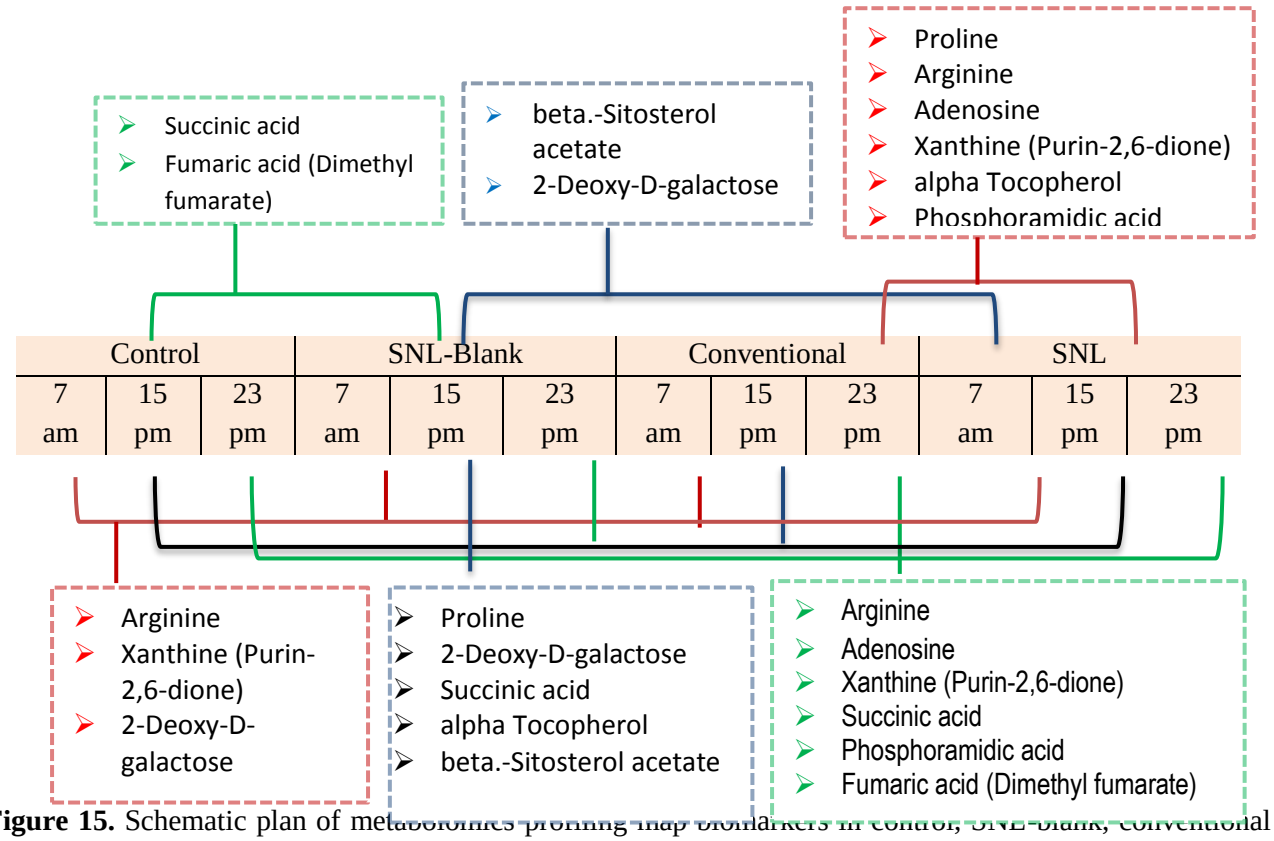

Figure 15. Schematic plan of metabolomics profiling map biomarkers in control, SNL-blank, conventional $_{honey\ \&\ PDGF}$G, and SNL $_{honey\ \&\ PDGF}$ G

2.15. Discussion

2.15.1. Synergistic effect between $SNL_{Honey\text{-}PDGF}$ formulas wound closure time

The efficiency of drugs combinations as remedies complex of wound treatment was well proven with PDGF and honey formulated Nano form, The combinations strategies based on managed the reduced toxicity, maximized efficacy and alter pharmacokinetics represented by increased absorption rate and controlled *t*½ life according to small size increase duration of action via controlled slow sustain release-prolonged t½ life as compared with single dosage of honey or PDGF potencies (Cedergreen, 2014).

The results presented the synergism of SNL honey-PDGF represented the dressed synergized concentrations 50:20 (11.97:0.08%) had been superior values of indices of higher fold in linear healing rate mm/day, closure $t_{½}$ days, and closure velocity mm/day (10.625, 12.518, and 14.402) respectively than other combination concentrations, these may be attributed to associated with the mechanisms and accelerated mode of action in

phasic of healing managed increased closure of the wound. The site of the synergistic event of both Honey& PDGF occurred in wound phases that presumably associated with each at the same sit of action in different mechanisms via itemized as follows stimulated in fibroblasts and smooth muscle cells metabolic process for collagen and protein production for PDGF (Pastar *et al.,* 2014) and honey (Al-Mohana, 2012; Anis *et al*., 2021), At the first phase in inflammatory dramatic consequences were showed the maybe play a major role in reduced complication with wound healing by honey facilitated progress healing by PDGF that presumably act as antibacterial, anti-inflammatory, antioxidant, disinfectant, antifungal, antiviral and therapeutic properties (Abbas *et al*., 2010), this knowledge appeared facilitated for synergism with PDGF reduced complication faced PDGF and shorting line for started PDGF although the provocation between honey and PDGF at same sit and mechanistic orchestration effect on wound healing, both were working at different mechanisms, which were facilitated complementary mechanisms in the healing process (Martinotti *et al*., 2019).

For honey, own acid prime application increased the fibroblast proliferation at pH indeed by enhancing peroxide generation, and releasing pro-inflammatory cytokines (TNF, IL-1, and IL-6) and PGE2 during the inflammatory phase (Kim *et al.*, 2020), as well as the honey presumably reduced inflammation by arresting and delay bacterial cell cycle, oxidative cellular damage, and act as antioxidant activity as well as logical reduced acidic concentration- metabolite and that maintain neutral pH of the wound may be facilitated the PDGF work natural media act as consider one of the first factors secreted after an injury and promotes cellular reactions throughout phases of the wound healing process (Sinai, 2008; Combarros *et al*., 2020).

The proliferative phase releases oxygen from hemoglobin due to buffering nature of honey, and due to high osmotic pressure the granulation tissue formation and re-epithelialization were stimulation, the wound edges were contracted, lowers exudate and edema in the wound, the low levels of hydrogen peroxide may be led to stimulating the development of new vessels and proliferation, growth of fibroblasts and epithelial cells in wound tissue (Almasaudi, 2021) that accelerated the time of healing and promote synergized via reducing time and permeation PDGF work at the application of PDGF via binding to specific receptors on cell membranes of target cells. The upregulation of TGF-beta production led to collagen formation, and insulin-like growth factor-1 synthesis (Cross and Mustoe, 2003).

Finally, the remodeling phase, for honey collagen was remodeled and realigned along tension lines, and cells no longer needed to be removed by apoptosis, as well as, the honey aids to reshape the wound, contractures and prevents scarring also to enhancement MMP-9, TGF-β, and hygroscopic impact during the proliferative and remodeling phases. Further synergism was promoted and achieved at the time of phase and encouraged each honey to PDGF at the remodeling phase (Oryan *et al.*, 2016).

For PDGF, the wound contraction, the formation of granulation tissue, and wound remodeling, according to Kalashnikova *et al*. (2015) agreed with our results show SNL is useful at various stages of wound healing based on the findings, most SNL improved wound healing by increase proliferation phase and inflammation phase, whereas only a few SNL are known to help in homeostasis and remodeling. Also, in another study, Homaeigohar and Boccaccini, (2020) reported the mechanisms for the antibacterial NPs facilitated tissue repair and were rarely able to efficiently resolve both wound healing and disinfection problems. As a result, they need to include bactericidal and healing-promoting functional agents to overcome this problem, newer honey-impregnated dressings lead in SNL were introduced (Halah and Hussein, 2018; Rosidi Sujanto *et al.*, 2021).

2.15.2. The chronotherapeutic challenge of synergistic $SNL_{Honey\ and\ PDGF}$ formulas on deep skin wounds

The results accumulated synergism Chrono effect with synergized SNL formulas (11.97: 0.08) for optimized the outcomes in wound closure efficiency, the phenomenon of circadian rhythms was derived from ubiquitous Chrono therapeutic phenomenon that managed facilitator fluctuation of internal homeostasis and orchestrated reflect on time administration of the drug influences optimizing therapeutic effect and reduced

side effect with maintains physiological regulation mechanistic cascade, as well as provide rhythms of function adapted and anticipate genomic coding express interact with circadian rhythm-tissue rhythmicity function (AI Mohammed and Al-Bayati, 2014; Wang *et al*., 2020).

The result showed the blank has negatively correlated with melatonin as well as the no correlation was in both $SNL_{Honey\&PDGF}$ and conventional $_{Honey\&PDGF}$ of linear healing rate. This result was attributed to the melatonin-circadian rhythm reflecting on normal physiological healing due to increase epithelialization of deposit and proliferation fibroblast may be due to direct motivation lamellipodia formation, which was proposed the molecular mechanism was a direct relationship between increased Per2 at dark mode with high melatonin concentration in the blood associated with cellular mobilization increase linear closure rate of skin wound, this suggestion of wound healing no correlation in $SNL_{Honey\&PDGF}$ and conventional $_{Honey\&PDGF}$ has coincided with the result of closure velocity and $t_{1/2}$ of closure time (Hoyle *et al.,* 2017). On the other hand, the result may be due to keratinocyte synchronization with diurnal sidle cell-intrinsic differentiation or increased response to melatonin turnover, which Janich *et al.,* (2011) suggested transcription-modulated mechanism in the early morning to evening complain from increased cell differentiation and proliferation.

The $SNL_{Honey\&PDGF}$ and $conventional_{Honey\&PDGF}$ do not correlate melatonin diurnal changes with indices of wound healing due to the healing tended to the type of treatment rather than synergistic with circadian rhythm, the result showed a direct effect in healing indices that may be due to the cortisol having to induce Krüppel-like factor 9 (KLF_9) expression, the KLF_9 has up-regulated expression at the morning, which was indirectly increased cell differentiation on the other hand there did not correlate with the circadian rhythm on healing may be due to was not get correlation cortisol with melatonin except control that gives the impression the circadian rhythm was not direct demand there synergistic effect with chrono-therapy at cortisol levels (Sporl *et al*., 2012).

Both the SNL-blank and $conventional_{Honey\&PDGF}$ have positively correlated cortisol with linear indices, whereas negatively correlated in all indices of $SNL_{Honey\&PDGF}$ treated groups that main the cortisol has negatively proportion with the healing process of $SNL_{Honey\&PDGF}$ with except and negatively with closure $t_{1/2}$ in conventional $_{Honey\&PDGF}$ (Ebrecht *et al.,* 2004).

For this reason of motivation wound healing via regulation of cortisol levels during the Chrono-therapeutics concerning healing, the cortisol levels during diurnal schedule displayed at 7 and 15 was higher than 23 in a day time in control and treated groups; conventional $_{Honey\&PDGF}$ and SNL $_{Honey\&PDGF}$ that may be governed the activity of wound healing processes increased at 23 alike in wound healing indices increases closure recovery with proportional with cortisol serum concentration. The $SNL_{Honey\&PDGF}$ treated rabbits' linear healing rate and closure velocity were negatively correlated with cortisol and the healing dramatic events were provoked between the Nano form of treatment and chrono-dark-night mode, whereas the control and $conventional_{Honey\&PDGF}$ treated rabbits were contrast results displayed a positive correlation between cortisol serum levels and both linear rate and velocity of closure of wounds may be controlled their effect direct with affecting of cortisol as an anti-inflammatory on the healing supposed act as accelerated wound closure depends on body participant synergized with healing for a short of inflammatory phase and dependency correlation depended on the cortisol in the conventionally treated group was lower than control and maybe another causal was endorsed in the healing, which was excreted that negative correlation between cortisol and $t_{½}$ closure in conventionally treated wounds maybe presumably delayed time of healing. Managed positively cortisol has previously been mentioned as delaying wound recovery (Goiun *et al.,* 2008). The Chrono set of therapeutic suggested the honey was provoked by the normal physiological aspect of cortisol inhibition pathways that give increased healing at night mood as well as associated with antagonized melatonin to the cortisol releasing (Ebrecht *et al.*, 2004).

The growth hormone has a result have all the schematic of correlation that approved the exogenous epidermal growth factor (EGF) application on the wound was neglected or canceled the endogenous growth

factor, despite there were highly correlated between growth hormone with melatonin but that maybe provoked growth hormone with at night mood and synergized wound healing via melatonin secretion in nigh, which improved wound healing via potential effects on the immune system coinciding with the secretion of GH during at the night this effect on the progression of wound healing during the night (Pugazhenthi *et al.*, 2008), Insulin was decreased at night mood at 23, while in control have a positive correlation between wound healing indices and insulin in moderate values in closure velocity and high in linear healing that may be attributed presumably to the insulin promotion re-epithelialization of injurious tissue that maybe motivation the migration and proliferation of keratinocyte as well as stimulate endothelial cell formation tube (Yang *et al.*, 2020) as well as insulin had to increase the ability of fibroblast deposition of collagen and fiber as well as forming a basket weave with reduced scar tissue that promotion increase reduced time of remodeling and increase remodeling quality during healing, whereas that negatively correlation with at $SNL_{Honey\&PDGF}$ due to the insulin was induced inflammatory phenomenon due to increase intensity inflammatory phase (Zhu *et al*., 2020).

But in control have a highly positive correlation between melatonin and insulin and a positive correlation in moderate values in $conventional_{Honey\&PDGF}$ and $SNL_{Honey\&PDGF}$ that can be attributed presumably to the mechanism of insulin-impaired wound healing via inflammatory phase maybe liberation of reactive oxygen species (ROS) and promotion of early infiltration through activation chemotactic effect via chemo-attractant protein-1 (MCP-1) expression, the reduction of insulin that prevent up-regulation of the inflammatory process (Azevedo *et al.*, 2016).

The remarkable result in thyroid stimulating hormone (TSH) correlation with linear healing have absent of correlation with all indices of wound healing but the control showed a correlation with linear as compared with control closure velocity and $t½$ that may be due to the several evidence the thyroid stimulating hormone to have a role in wound healing via expression of their receptor in epidermal, dermal fibroblast and keratinocyte, which suggested induced proliferation of keratinocytes and fibroblasts via up-regulation keratinocyte intracellular c.AMP (Nie *et al.*, 2014).

2.15.3. Role protein and DNA in wound healing

The healing process of soft tissue in the wound is a complex orchestration of cellular recovery and differentiation, the protein and DNA quantity, and internal marker factors, which may be increased the protein and DNA, and have a diagnostic and predictive enhancement for the status of wound healing. The results showed a marked increase of protein concentration in $SNL_{Honey\&PDGF}$ in the growth phase and remodeling phase at 23 set times, this was managed presumably due to the two-factor type of treatment dominancy of $SNL_{Honey\&PDGF}$ on other treatments and second diurnal effect. The $conventional_{Honey\&PDGF}$ was an accelerated healing deposit of granulation tissue and cellular layers with increased linear healing rate and closure velocity at 23 treated wounds, as well as decreased $t_{½}$ that give imbrication that building unit increase protein, our results agreed with Janis and Harrison (Janis and Harrison, 2016) which attributed the protein deposition in multiple phases has building blocks of soft tissue in the skin that derived from the diurnal cell as the unit of repair throughout the process of wound healing.

The protein during healing may be derived from RNA-DNA up-regulation synthesis agreed with our results that increase DNA quantities in $SNL_{Honey\&PDGF}$ as compared with other groups, as well as the protein was higher than in the remodeling phase in the growing phase suggested due to the amount of protein as a tissue compound in growing phase than remodeling phase, in other words, the area of closure wound increased over time and accelerated the induction of opening that showed a quantitative analysis of protein was conceded with healing indices of the wound. The results showed not an obvious correlation between diurnal set time protein synthesis presumably the healing process of cellular deposition affected by an external

therapeutic agent than that diurnal time was as mainly affected on $SNL_{Honey\&PDGF}$ correlation may be due to the $SNL_{Honey\&PDGF}$ within the time accelerated proliferation at nigh mode therapy (Dryden *et al.,* 2013).

The DNA in conventional high correlated with closure t½ negatively and less in velocity and linear healing rate positively that maybe direct effecting of DNA quantity growing phase and increase cell proliferation that the healing process indices was in conventional $_{Honey\&PDGF}$ was have DNA dependent other than protein quantity presumably due to cell proliferation and less matrix deposition were as in remodeling as same at in conventional$_{Honey\&PDGF}$ relationship with DNA quantity in both closure *t*½, velocity and linear healing rate dependency on functional DNA on indices of wound processing healing (Rodrigues *et al.,* 2019).

The DNA increase cell proliferation which increased the deposition of healing material due to the up-regulation of DNA synthesis (Weimann *et al.,* 2017). Collagen synthesis and elastic tissue formation, immune system accelerated function as well as epidermal growth that which were post the treated growth factor than increase keratinization-proteoglycan deposition, Both DNA and protein synthesis accelerated the healing process by amino acid and oligopeptides forming unit of healing block, as well as honey and growth factors may be caused promotion of DNA methylation, acetylation, phosphorylation, and adenylation via controlling histone phosphatases and kinases enzyme phosphorylation that regulated transcription and DNA repair and decrease cell member deposition (Yan *et al*., 2018).

2.15.4. Metabolomics in wound healing

The metabolome analysis result facilitated the detection of more than 206 metabolome drive features of Chrono therapeutic time point (7,15, and 23), which allows screening of how the deep excisional wound metabolomes altered across Chrono. The metabolomics marker of arginine was a marker of the high rate of wound healing in treated groups in conventional at 7 and 23 and SNL at 23 arginine is one of the essential amino acids modulated due to the angiogenesis endothelial function and implicated in immune function (Campos *et al.,* 2008). Malone-Povolny *et al.* (2017) reported that arginine has a major in the wound healing process, the arginine produced polyamine ornithine-proline via arginase I pathway, and the polyamines were attributed to provoked cell proliferation as well as collagen synthesis, furthermore; the metabolism of arginine derived inducible nitric oxide via nitric oxide synthesis which directly has an archive of role in the healing of wound which was suggested regulate the proliferation of cell and collagen formation as well as wound contraction (narrowing of the wound) (Barchitta *et al.,* 2019).

Fumaric acid markers control at time 23 one of the endogenous materials exert in the induction of wound and wound healing have a role in the mechanical ability to restore cutaneous lymphocyte and in the innate inflammatory responses via inhibiting nuclear factor kappa B (NF-κB) activation that play improvement wound healing in different condition(Nicolay *et al.,* 2021).

The fumaric acid provoked NRF2 antioxidant signaling that accelerated wound healing especially in keratinocytes cell plays a protective effect and this consider a compensatory mechanism of cell defense in response to cutaneous injury. The NRF2 antioxidant signaling is activated in response to low basal free radicals, and scavenging of ROS led to averting oxidative damage and inflammatory prognosis. In addition, fumaric acid can increase fibroblast proliferation, collagen synthesis, granulation tissue formation, and angiogenesis (Dunnill *et al.,* 2017).

The adenosine one of the markers $SNL_{Honey\&PDGF}$ at time 23 which acts as an identifier to progress well wound tissue healing and augmented between wound metabolic process of the wound healing process, Gontcharova *et al,* (2010) suggested that the abundance plenty of adenosine may be referred to wound maturity.

Well-known result the healing response was achieved mainly in $SNL_{Honey\&PDGF}$ at 23 as well as less healing at 7, the identity of xanthine the related compound has an appositive indication of wound hydration (Stewart

and Costerton, 2001), especially in the epidermis layer. Hydration is a success factor for healing closure and reducing scar-forming and wet entities in the skin.

The SNL-blank treatment distinguished by 2-Deoxy-D-galactose at times 7, 15, this is associated with excessive forming of extracellular matrix and collagen deposition that maybe en dose 2-Deoxy-D-galactose in biochemical turnover during granulation tissue accumulation(Howell-Jones *et al.*, 2005).

The result is a metabolite of Phosphoramidic acid of the marker $SNL_{Honey\&PDGF}$ at time 23 which is a precursor of phosphorus in wound healing, the acidification cell microenvironment due to metabolic activity that immortalized keratinocytes and activated fibroblast that plays a vital role for cell division their growth in new tissue and development (Yang *et al*., 2021).

The bad prognosis of healing in conventional at 15 than SNL was identified proline amino acid as metabolite ornithine with a basic of collagen-building forming granuloma and fibrosis that healing bad prognosis, the remodeling was a delay and insufficient and maybe change the wound form acute to the chronic wound, this increase extracellular matrix synthesis both arginine, proline mediated ornithine pathway maybe a mechanistic correlation between the type of inflammation and bad prognosis fibrosis (Budi *et al.*, 2021).

The succinate one of the markers SNL- blank at 23 and control at 15, succinate is derived from a-ketoglutarate through succinyl-CoA which is converted to fumarate via succinate dehydrogenase, direct succinate dehydrogenase inhibition appears to be a vital role to treat impaired healing conditions. There is a clear correlation between succinate and inflammation that has been influenced by an inflammatory response that regulates inflammation, dysregulated succinate metabolism plays an important role in maintaining the chronic wound environment (Ryan *et al.*, 2019).

The SNL base component in the blank at 15 has a marker identifying β-sitosterol acetate which is important for healing as well as occurring of honey and PDGF the β-sitosterol was exerted as a biomarker of blank treated with SNL, which indication of mimics proliferation, and migration of fibroblast that may give an indication the SNL formula have synergistic with their content as well as SNL in wound healing (Al-Roujayee, 2017).

The α-tocopherol as named vitamin E was identifying metabolomics biomarker of SNL at 15 which plays an antioxidant property endogenously changes during time vibration during circadian rhythm time which directly as an alternative pathway to survival healing mechanism via direct correlation with growth factor expression in connective tissue and facilitated wound healing protection (Pierpaoli *et al*., 2011).

2.16. Conclusion

Structure Nano lipid has different advantages in delivery systems for topical application and accelerated wound healing. The $SLN_{Honey\&\ PDGF}$ increased of synergism of honey and PDGF and therefore increased the chance of wound healing in a short time. The Chrono-therapeutic effect challenge led to optimized outcomes that were set at a certain time of treatment to increase the efficiency of the therapeutic effect via utilizing circadian rhythm. This unique exploratory study successfully demonstrates the temporal and dynamic acute wound metabolome whilst also was helped to identify a class of biomarkers that correspond to wound healing processes.

2.17. Recommendations

An Extension of the idea of developing and surveying activities of Honey and PDGF in Nano form on the body is assumed as follows:

1. Clinical usage of a new formulation of $SNL_{Honey\&\ PDGF}$ in the wound of large animals.
2. Although circadian rhythm interactions at the cellular level seem very easily detectable, there is always a physiological undercurrent that may influence the outcomes, which can create a favorable or unfavorable environment for regeneration. Determination of molecular events at the chronotherapeutic period
3. Highlights the need for further research into skin sensitivity and reaction via explored metabolomics.

REFERENCES

Monika, P., Waiker, PV., Chandraprabha, MN., Rangarajan, A. and Murthy, KNC. 2021. Myofibroblast progeny in wound biology and wound healing studies. Wound Repair Regen, 29(4): 531–547.

Campos, J.R., Severino, P., Santini, A., Silva, A.M., Shegokar, R., Souto, S.B. and Souto, E.B. 2020. Chapter 1-Solid lipid nanoparticles (SLN): Prediction of toxicity, metabolism, fate and physicochemical properties. In Nanopharmaceuticals; Shegokar, R., Ed.; Elsevier: Amsterdam, The Netherlands, pp. 1–15.

Araujo, V.H.S., Delello Di Filippo, L., Duarte, J.L., Spósito, L., de Camargo, B.A.F., da Silva, P.B. and Chorilli, M. 2020. Exploiting solid lipid nanoparticles and nanostructured lipid carriers for drug delivery against cutaneous fungal infections. Crit. Rev. Microbiol, 47(10): 79–90.

Devdhawala, MG. and Seth, AK. 2010. Current status of Chronopharmatherapeutic drug delivery system: an overview. J Chem. Res, 2(3): 312-328.

Zhang, J., Xiao, X. and Zhu, J. 2018. Lactoferrin-and RGD-comodified, temozolomide and vincristine-coloaded nanostructured lipid carriers for gliomatosis cerebri combination therapy. Int J Nanomedicine. 13(1): 3039-3051.

Nawal, S. Jaafer, Balqees, H.A., Mohanad, A. Al-Bayati. 2020. Preparation and Standardization of Liposomes Encapsulated Newcastle Disease Vaccine in Unilamellar and multilamellar forms. Plant Archives., 20(1): 978-982.

Buthina, A Abdullaha, Mohanad, A AL-Bayati. 2023. Production and Characterization of Nanostructured-Lipid Carriers as Hormones PGF2αand PMSG. The Egyptian Journal of Hospital Medicine, 90(1): 412-420.

Roaa K J, Mohanad A. Al-B. 2022. preparation and standardization of structural Nano-lipid loaded lidocaine and conventional lidocaine. International Journal of Health Sciences, 2(3):18-21.

Berenbaum, M.C. 1989. What is synergy? Pharmacological Reviews, 41(2): 93-141.

Ali, M. Ghazi and Mohanad, A Al-Bayati. 2020. Anti-proliferative of the phytosome propolis, phytosome lycopene and synergistic effect on the benign prostatic hyperplasia cells in-vitro. Plant Arch., 20(1): 6579-6589.

Poch, G. and Holzmann, S. 1980. Quantitative estimation of overadditive and underadditive drug effects by means of additive dose- response curves. Journal of pharmacological Methodes, 4(2): 179-188.

Balbino, C.A., Pereira, L.M. and Curi, R. 2005. Mechanisms involved in wound healing: arevision. Rev Bras Cienc Farm., 41(1): 27-51.

Camila, D., Carolina, C., and Marcelo, S. 2015. Time-resolved and steady-state fluorescence spectroscopy for the assessment of skin photoaging process. Journal of SPIE digital library, 5(1): 44-48.

Bruno, W., Laura, Z., and Guilherme, G. 2020. Topical application of lidocaine or bupivacaine in the healing of surgical wounds in dogs. Journal of Acta Cirurgica Brasileira, 32(12):23-25.

Gopinath, D., Ahmed, M. R., Gomathi, K., Chitra, K., Sehgal, P.K. and Jayakumar, R. 2004. Dermal wound healing processes with curcumin incorporated collagen films. Journal of Biomaterials, 25(10): 1911-1917.

Cassini-Vieira, P., Moreira, C. F., da Silva, M. F. and Barcelos, L. S. 2015. Estimation of wound tissue neutrophil and macrophage accumulation by measuring myeloperoxidase (MPO) and N-Acetylβ-D-glucosaminidase (NAG) activities. Journal of Bio-protocol, 5(22): e1662.

Roaa K J, Mohanad AAl-Bayati. 2022. Preparation and standardizations of structural nano- lipid loaded lidocaine and conventional lidocaine. International Journal of Health Sciences, 6(S1): 14145-14156.

Gilman T. 2004. Wound Outcomes: The Utility of Surface Measures. The International Journal of Lower Extremity Wound, 3(3): 125-132.

Vidal, X., Cheung, S. and Chiapolini, N. 2015. Observation of J/ψp Resonances Consistent with Pentaquark States in Λ0b→J/ψK−p Decays. Journal of Physical Review Letters., 33(14): 32-36.

Lowry, O. H., Rosebrough, N.J., Farr, AL. and Randal, R.J. (1951). Protein measurement with the folin phenol reagent. J. Biol. Chem., 193(1): 265-275.

Sambrook, J. and Russell, DW. 2001. In: Molecular Cloning: A Laboratory Manual, 3rd edition, Cold Spring Harbor Laboratory Press. NY., 7(4): 7-8.

Li Han,T., Yang, Y., Zhang, H. and Law, K.P. 2017. Analytical challenges of untargeted GC-MS-based metabolomics and the critical issues in selecting the data processing strategy. F1000 Research. 6(1): 967.

Maurya, K. 2012. Chronopharmacology: A tool for therapy of diseases.IRJP., 3(5): 128-132.

Evans, WS., Rogol, AD., MacLeod, RM. and Thorner, MO. 1980. Dopaminergic mechanisms and luteinizing hormone. Secretion: I. Acute administration of the dopamine agonist bromocriptine does not inhibit luteinizing hormone release in hyperprolactinemic women. J Clin Endocrinol Metab., 50(1): 103-107.

Hepburn, S., Farid, S., Dawson, J. and Goodall, S. 2012. Thyroid function testing. British Journal of Hospital Medicine. Br J Hosp Med (Lond)., 73(8): 114-118.

Roberts, RF. and Roberts, WL. 2004. Performance characteristics of five automated serum cortisol immunoassays. Clin Biochem; 37(6): 489–493.

Li, X.F., Liu, Y., Zhang, J., You, R.C., Qu, J. and Li, M.Z. 2017. Functionalized silk fibroin dressing with topical bioactive insulin release for accelerated chronic wound healing, Mat. Sci. Eng. C-Mater., 72(1): 394-404.

Armitage, P. and Berry, G. 1994. In: Statistical Methods in Medical Research, 3rd edn. Oxford: Black well Scientific Publications, 312- 341.

Trezzi, J.P., Jäger, C., Galozzi, S., Barkovits, K., Marcus, K., Mollenhauer, B. and Hiller, K. 2017. Metabolic profiling of body fluids and multivariate data analysis. MethodsX. 4(1): 95-103.

Ali, M G. and Mohanad, A Al-B. 2019. Metabolomic profiling of Iraqi propolis Samples Collected from Al-Diwanyiah city. Al-Qadisiyah Journal of Veterinary Medicine Sciences, 18(2).

Fiehn, O. and Kind,T. 2005. Metabolite profiling in blood plasma. Oliver Fiehn and Kind book ,chapter metabolomics.

Jassim, S.J. and Al-Bayati, MA. 2019. Plasma metabolomics in mice gavaged aspirin with or without liposome during luteal and follicular phases. Online Journal of Veterinary Research, 23(9): 852-872.

Al-Bayati, M.A. and Khames, W. 2015. Importance of following standardized guideline for the care and use for laboratory animals in research and teaching in Iraqi scientific institutions FIQ. J. Med. Sci., 2: 11-14.

Tome O. H. 2009. Comparaision of calibration curve fitting methods in absorption spectroscopy, Anal. Chem., 1976(48): 312-318.

Cedergreen, N. 2014. Quantifying synergy: A systematic review of mixture toxicity studies within environmental toxicology. PLoS One 9(5): e96580.

Pastar, I., Stojadinovic, O., Yin, N.C., Ramirez, H., Nusbaum, A.G., Sawaya, A., Patel, S.B., Khalid, L., Isseroff, R.R. and Tomic-Canic, M. 2014. Epithelialization in Wound Healing: A Comprehensive Review. Adv. Wound Care, 3(7): 445-464.

Anis, A., Sharshar, A., El Hanbally, S. and Sadek, Y. 2021. A Novel Organic Composite Accelerates Wound Healing: Experimental and Clinical Study in Equine. J. Equine Vet. Sci., 99(3): 103406.

Martinotti, S., Bucekova, M., Majtan, J. and Ranzato, E. 2019. Honey: An Effective Regenerative Medicine Product in Wound Management. Curr. Med. Chem., 26(27): 5230-40.

Kim, N., Choi, K.U., Lee, E., Lee, S., Oh, J., Kim, W.K., Woo, S.H., Kim, D.-Y. Kim, W.-H. and Kweon, O.-K. 2020. Therapeutic effects of platelet derived growth factor overexpressed-mesenchymal stromal cells and sheets in canine skin wound healing model. Histol. Histopathol., 35(7): 751-767.

Combarros-Fuertes, P., Fresno, J.M., Estevinho, M.M., Sousa-Pimenta, M., Tornadijo, M.E. and Estevinho, L.M. 2020. Honey: Another alternative in the fight against antibiotic-resistant bacteria? Antibiotics, 9(11): 774.

Almasaudi, S. 2021. The antibacterial activities of honey. Saudi J. Biol. Sci., 28(4): 2188-2196.

Cross, K.J. and Mustoe, T.A. 2003. Growth factors in wound healing. Surg. Clin. N. Am., 83(3): 531-545.

Oryan, A., Alemzaden, E. and Moshiri, A. 2016. Biological properties and therapeutic activities of honey in wound healing: A narrative review and meta-analysis, Journal of Tissue Viability, 25(2): 98-118.

Kalashnikova, I., Das, S. and Seal, S. 2015. Nanomaterials for wound healing: Scope and advancement. Nanomedicine, 10(16): 2593-2612.

Homaeigohar, S. and Boccaccini, A.R. 2020. Antibacterial biohybrid nanofibers for wound dressings. Acta Biomater., 107(1): 25-49.

Rosidi Sujanto, I.S., Ramly, N.S., Abd Ghani, A., Tang Yew Huat, J., Alias, N. and Ngah, N. 2021. Composition and functional properties of stingless bee honey: A review. Malays. J. Appl. Sci., 6(1): 111-127.

AI Mohammed and Al-Bayati, MA. (2014). Comparative study among watermelon crud extract, citrulline and lycopene on some reproductive indices in male mice. International Journal of Research, 3(6): 2307-2083.

Wang, H., Yang, Z., Li, X., Huang, D., Yu, S., He, J., Li, Y. and Yan, J. 2020. Single-cell in vivo imaging of cellular circadian oscillators in zebrafish. PLoS Biol 18(3): e3000435.

Hoyle, N.P., Seinkmane, E., Putker, M., Feeney, K.A., Krogager, T.P., Chesham, J.E., Bray, L.K., Thomas, J.M., Dunn, K. and Blaikley, J. 2017. Circadian actin dynamics drive rhythmic fibroblast mobilization during wound healing. Sci. Transl. Med., 9(415): eaal 2774.

Janich, P., Pascual, G., Merlos-Suárez, A., Batlle, E., Ripperger, J., Albrecht, U., Cheng, H.Y.M., Obrietan, K., Di Croce, L. and Benitah, S.A. 2011. The circadian molecular clock creates epidermal stem cell heterogeneity. Nature, 480(7376): 209-214.

Sporl, F., Korge, S., Jurchott, K., Wunderskirchner, M., Schellenberg, K., Heins, S., Specht, A., Stoll, C., Klemz, R. and Maier, B. 2012. Kruppel-like factor 9 is a circadian transcription factor in human epidermis that controls proliferation of keratinocytes. Proc. Natl. Acad. Sci. USA, 109(27): 10903-10908.

Ebrecht, M., Hextall, J. and Kirtley, L-G. 2004. Perceived stress and cortisol levels predict speed of wound healing in healthy male adults. Psychoneuroendocrinology., 29(6): 798-809.

Goiun, JP., Kiecolt-Glaser, JK. and Malarkey, WB. 2008. Influence of anger on wound healing. Brain Behav Immun., 22(55): 699-708.

Ebrecht, M., Hextall, J. and Kirtley, L-G. 2004. Perceived stress and cortisol levels predict speed of wound healing in healthy male adults. Psychoneuroendocrinology., 29(6): 798-809.

Pugazhenthi, K., Kapoor, M., Clarkson, AN., Hall, I. and Appleton, I. 2008. Melatonin accelerates the process of wound repair in full-thickness incisional wounds. Journal of Pineal Research, 44(4): 387-396.

Yang, S., Zhang, Y., Zhang, Z., Dan, J., Zhou, Q., Wang, X., Li, W., Zhou, L., Yang, L. and Xie, L. 2020. Insulin promotes corneal nerve repair and wound healing in type 1 diabetic mice by enhancing Wnt/beta-catenin signaling, Am. J. Pathol., 190(11): 2237-2250.

Zhu, J., Jiang, G., Hong, W., Zhang, Y., Xu, B., Song, G., Liu, T., Hong, C. and Ruan, L. 2020. Rapid gelation of oxidized hyaluronic acid and succinyl chitosan for integration with insulin-loaded micelles and epidermal growth factor on diabetic wound healing, Mater. Sci. Eng. C-Mater. Biol. Appl., 117(7): 111273.

Azevedo, F., Pessoa, A., Moreira, G., Santos, M.D., Liberti, E., Araujo, E., Carvalho, C., Saad, M. and Lima, M.H. 2016. Effect of topical insulin on second-degree burns in diabetic rats, Biol. Res. Nurs., 18(2): 181-192.

Nie, C., Yang, D., Liu, N., Dong, D., Xu, J. and Zhang, J. 2014. Thyrotropin-releasing hormone and its analogs accelerate wound healing. J. Surg. Res., 189(2): 359-365.

Janis, J.E. and Harrison, B. 2016. "Wound healing," Plastic and Reconstructive Surgery, 138(3): 9S-17S.

Dryden, S.V., Shoemaker, W.G. and Kim, J.H. 2013. "Wound management and nutrition for optimal wound healing," Atlas of the Oral and Maxillofacial Surgery Clinics., 21(1): 37-47.

Rodrigues, M., Kosaric, N., Bonham, C. A., and Gurtner, G. C. 2019. Wound healing: A cellular perspective. Physiol. Rev., 99(1): 665-706.

Weimann, A., Braga, M. and Carli, F. 2017. "ESPEN guideline: clinical nutrition in surgery," Clinical Nutrition, 36(3): 623-650.

Yang, L., Zhang, D., Wu, H., Xie, S., Zhang, M. and Zhang, B. 2018. Basic Fibroblast Growth Factor Influences Epidermal Homeostasis of Living Skin Equivalents through Affecting Fibroblast Phenotypes and Functions. Skin Pharmacol Physiol, 31(5):229-37.

Campos, A.C.L., Groth, A.K. and Branco, A.B. 2008. Assessment and nutritional aspects of wound healing. Curr. Opin. Clin. Nutr. Metab. Care, 11(3): 281-288.

Malone-Povolny, M.J., Maloney, S.E. and Schoenfisch, M.H. 2019. Nitric Oxide Therapy for Diabetic Wound Healing. Adv. Healthc. Mater., 8(12): e1801210.

Barchitta, M., Maugeri, A., Favara, G., San Lio, R.M., Evola, G., Agodi, A. and Basile, G. 2019. Nutrition and wound healing: An overview focusing on the beneficial effects of curcumin. Int. J. Mol. Sci., 20(5): 1119.

Nicolay, J.P., Albrecht, J.D., Assaf, C., Dippel, E., Stadler, R., Wehkamp, U., Wobser, M., Guelow, K., Goerdt, S. and Krammer, P.H. 2021. Dimethyl fumarate (DMF) therapy in CTCL: Results from a clinical phase II study. Eur. J. Cancer, 156(1): S21-S22.

Dunnill, C., Patton, T., Brennan, J., Barrett, J., Dryden, M., Cooke, J., Leaper, D. and Georgopoulos, N.T. 2017. Reactive oxygen species (ROS) and wound healing: The functional role of ROS and emerging ROS-modulating technologies for augmentation of the healing process. Int. Wound J., 14(1): 89-96.

Halah, M. and Hussein, AL-Hasani. 2018. Study Antibacterial Activity of Honey Against Some Common Species of Pathogenic Bacteria. Iraqi Journal of Science, 59(1A): 30-37.

Gontcharova, V., Youn, E., Sun, Y., Wolcott, RD. and Dowd, SE. 2010. A comparison of bacterial composition in diabetic ulcers and contralateral intact skin. Open Microbiol J., 4(1): 8-19.

Stewart, PS. and Costerton, JW. 2001. Antibiotic resistance of bacteria in biofilms. Lancet., 358(9276): 135-138.

Howell-Jones, RS., Wilson, MJ., Hill, KE., Howard, AJ., Price, PE. and Thomas, DW. 2005. A review of the microbiology, antibiotic usage and resistance in chronic skin wounds. J Antimicrob Chemother., 55(2): 143-9.

Abbas, H.N. Al-saeed, Saffaa, A.A. and Ali, A. Abed Al-abbas. 2010. Inhibitory effect of local Honey on Bacteria in culture media and in laboratory animals. The Iraqi Journal of Veterinary Medicine, 34(1): 103-110.

Yang, Q., Liang, H., Maulu, S., Ge, X., Ren, M., Xie, J. and Xi, B. 2021. Dietary phosphorus affects growth, glucolipid metabolism, antioxidant activity and immune status of juvenile blunt snout bream (Megalobrama amblycephala). Anim. Feed Sci. Technol., 274(2): 114896.

Budi, E.H., Schaub, J.R., Decaris, M., Turner, S., and Derynck, R. 2021. TGFb as a driver of fibrosis: physiological roles and therapeutic opportunities. J. Pathol., 254(4): 358-373.

Ryan, D.G., Murphy, M.P., Frezza, C., Prag, H.A., Chouchani, E.T., O'Neill, L.A., and Mills, E.L. 2019. Coupling Krebs cycle metabolites to signalling in immunity and cancer. Nat Metab., 1(2): 16-33.

Al-Roujayee, AS. 2017. Naringenin improves the healing process of thermally-induced skin damage in rats. J Int Med Res., 45(2): 570-582.

Al-Mohana, A.M.G. 2012. Biological activity of local honey bees in growth of some gram positive and negative bacteria, The Iraqi Journal of Veterinary Medicine, 36(1): 15-24.

Pierpaoli, E., Cirioni, O., Barucca, A., Orlando, F., Silvestri, C., Giacometti, A. and Provinciali, M. 2011. Vitamin E supplementation in old mice induces antimicrobial activity and improves the efficacy of daptomycin in an animal model of wounds infected with methicillin-resistant Staphylococcus aureus. J Antimicrob Chemother., 66(9): 2184-2185.

Sinai Waleed, 2008. THE ACTIVITY OF NATIVE NONEY AGAINST SOME MICROORGANISMS, Iraqi Journal of Science, 49(1): 264-268.